REPORT DOCUMENTATION PAGE

Form Approved
OMB No. 074-0188

1. AGENCY USE ONLY (Leave blank)	2. REPORT DATE	3. REPORT TYPE AND DATE COVERED
	7 May 2007	

4. TITLE AND SUBTITLE
Multi-pulse Converters and Passive Filtering to Improve Power Harmonics in an Integrated Power System

5. FUNDING NUMBERS

6. AUTHOR(S)
Ku, Daniel C.

7. PERFORMING ORGANIZATION NAME(S) AND ADDRESS(ES)		8. PERFORMING ORGANIZATION REPORT NUMBER

9. SPONSORING/MONITORING AGENCY NAME(S) AND ADDRESS(ES)		10. SPONSORING/MONITORING AGENCY REPORT NUMBER
US Naval Academy Annapolis, MD 21402		**Trident Scholar project report no. 354 (2007)**

11. SUPPLEMENTARY NOTES

12a. DISTRIBUTION/AVAILABILITY STATEMENT	12b. DISTRIBUTION CODE
This document has been approved for public release; its distribution is UNLIMITED.	

13. ABSTRACT The United States Navy is considering new power distribution architectures for surface combatants to enhance war-fighting capabilities and ship design opportunities. One such concept is the Integrated Power System (IPS) in which a common electric bus delivers power to both the ship's propulsion system and ship service electric system. One of the main challenges to the IPS/all-electric ship is the introduction of significant harmonic distortion into the main AC distribution bus caused by power electronic equipment. Power electronic equipment is necessary to implement the variable-speed motor drive for propulsion and for power conversion associated with distribution. The harmonic distortion leads to derating distribution equipment and degrading the performance of various system loads. As a result, every system attached to the main distribution bus must be able to accommodate the harmonics or the harmonics must be reduced to acceptable levels.The project's objective is to compare competing strategies that seek to reduce bus harmonics in a naval warship IPS. The subsidiary benefit of this task is to improve the efficiency and minimize the derating factor for shipboard engines, generators, and transformers. The proposed method of reducing harmonics is a system based on multi-pulse rectifiers and passive filtering. A multi-pulse rectifier is a power electronic device that converts AC power into DC power. Six and twelve-pulse rectifier systems are simulated and evaluated, as well as constructed and tested in the laboratory on a reduced scale. A design paradigm for passive filtering is set forth for each system. Size, weight, and acquisition cost estimates are derived from vendor data and assessed for feasibility of implementation on an actual destroyer-class warship. This project demonstrates the feasibility of improving power harmonics in an IPS using a system of multi-pulse converters and filtering.

14. SUBJECT TERMS	15. NUMBER OF PAGES
Total Harmonic Distortion (THD), Integrated Power System (IPS), Multi-pulse Converters (IPS), Power Harmonics, Harmonic Filter.	**72**
	16. PRICE CODE

17. SECURITY CLASSIFICATION OF REPORT	18. SECURITY CLASSIFICATION OF THIS PAGE	19. SECURITY CLASSIFICATION OF ABSTRACT	20. LIMITATION OF ABSTRACT

U.S.N.A. --- Trident Scholar project report; no. 354 (2007)

MULTI-PULSE CONVERTERS AND PASSIVE FILTERING TO IMPROVE POWER HARMONICS IN AN INTEGRATED POWER SYSTEM

by

Midshipman 1/c Daniel C. Ku
United States Naval Academy
Annapolis, Maryland

_____

Certification of Advisers Approval

Associate Professor John G. Ciezki
Electrical Engineering Department

_____

_____

Assistant Professor Thomas Salem
Electrical Engineering Department

_____

_____

Acceptance for the Trident Scholar Committee

Professor Joyce E. Shade
Deputy Director of Research & Scholarship

_____

_____

USNA-1531-2

Abstract

The United States Navy is considering new power distribution architectures for surface combatants to enhance war-fighting capabilities and ship design opportunities. One such concept is the Integrated Power System (IPS) in which a common electric bus delivers power to both the ship's propulsion system and ship service electric system.

One of the main challenges to the IPS/all-electric ship is the introduction of significant harmonic distortion into the main AC distribution bus caused by power electronic equipment. Power electronic equipment is necessary to implement the variable-speed motor drive for propulsion and for power conversion associated with distribution. The harmonic distortion leads to derating distribution equipment and degrading the performance of various system loads. As a result, every system attached to the main distribution bus must be able to accommodate the harmonics or the harmonics must be reduced to acceptable levels.

The project's objective is to compare competing strategies that seek to reduce bus harmonics in a naval warship IPS. The subsidiary benefit of this task is to improve the efficiency and minimize the derating factor for shipboard engines, generators, and transformers. The proposed method of reducing harmonics is a system based on multi-pulse rectifiers and passive filtering. A multi-pulse rectifier is a power electronic device that converts AC power into DC power. Six and twelve-pulse rectifier systems are simulated and evaluated, as well as constructed and tested in the laboratory on a reduced scale. A design paradigm for passive filtering is set forth for each system.

Size, weight, and acquisition cost estimates are derived from vendor data and assessed for feasibility of implementation on an actual destroyer-class warship. This project demonstrates the feasibility of improving power harmonics in an IPS using a system of multi-pulse converters and filtering.

Keywords

Total Harmonic Distortion (THD)

Integrated Power System (IPS)

Multi-pulse Converters

Power Harmonics

Harmonic Filter

Acknowledgements

I would like to thank Professor Ciezki and Professor Salem for their guidance and support with this project. Without them, this project would have been impossible. I would also like to thank the Electrical Engineering Department Lab Technicians for helping me set up equipment, providing technical support, and assisting whenever needed. I would also like to thank Bonnie Jarrell, the Electrical Engineering Department secretary, for always providing a smile and helping with the administrative side of this project. Finally, I would like to thank Professor Shade and the members of the Trident Scholar Committee for their continual dedication.

Table of Contents

List of Figures/Tables

Glossary

Apparent Power: "total" power; if the impedance of the system is purely resistive, the voltage and current are in-phase and apparent power is equal to real power; otherwise, it is equivalent to the magnitude of the phasor sum of real and reactive power

Diode: semiconductor device that operates in a manner similar to that of a mechanical check valve, carrying current in only one direction. A diode turns ON when it has a positive voltage across it; it turns OFF when the diode current attempts to reverse its direction (turn negative)

Filter: electronic circuit that rejects or passes a signal based on its frequency

Generator: rotating machine that converts mechanical energy into electrical energy; for a ship, a generator produces 3-phase AC power (same as synchronous machine)

Harmonic: a component frequency of a periodic signal that is an integer multiple of the fundamental frequency; i.e. if the fundamental frequency is 60Hz, the second harmonic is 120Hz

Inverter: power electronic device that converts DC power into AC power

Motor Drive: power electronic system that converts fixed-amplitude, fixed-frequency AC power into variable-amplitude, variable-frequency AC power to control a motor

Power Conversion Module: system that converts power into the appropriate form for distribution to various loads

Power Electronic Converter: a circuit that employs semiconductor devices in order to transform power from one form into another; i.e. from AC into DC

Power Factor: ratio of real power to apparent power, represented as a dimensionless number between 0 and 1

Prime Mover: gas turbine engine that converts fuel into mechanical power

Propulsion Motor: electric motor that drives the propeller, which in turn drives the ship

Reactive Power: "cost" of charging and discharging the magnetic fields of inductors and the electric field of capacitors

Real Power: "useful" power that is manifested in a tangible form, such as heat, light, or mechanical motion

Root Mean Square (RMS): the effective value of voltage or current; the waveform is squared, the result is averaged over time, and the square root of the value is taken

Ship Service: shipboard electrical power requirements not related to propulsion such as lighting, heating, and computers

Rectifier: power electronic device that converts AC power into DC power

Thyristor: controllable diode in which turn on can be delayed from its natural point

I. Introduction

The concept of integrated electric ship propulsion is popular in the U.S. Navy because it provides opportunities for new war-fighting capabilities and a flexible arrangement of equipment. An Integrated Power System (IPS) is one in which a common electric bus delivers power to both the ship's propulsion system and ship service electric system, as illustrated in Figure 1. The concept dates back to the early 1900s; however, modern IPS architectures exploit advancements in power electronics.

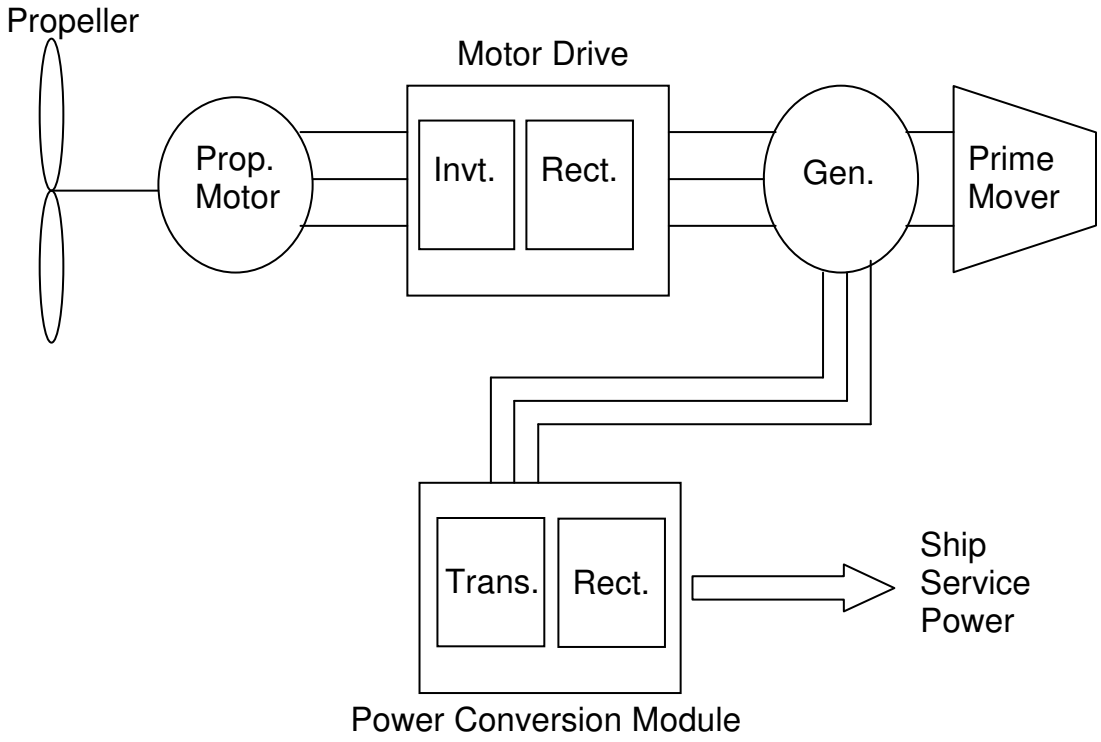

Figure 1: Integrated Electric Drive Ship[1]

In Figure 1, the prime mover is a mechanical engine that drives an AC synchronous generator, which would typically produce fixed-amplitude 60 Hz voltages. In the motor drive, the AC voltages are first converted to DC by a rectifier. Variable-frequency, variable-amplitude AC is then synthesized by a power electronic device called an inverter. The inverter output is

applied to a propulsion motor that is directly coupled to the propeller shaft. To enhance reliability and survivability, the propulsion motor will have more than the traditional three phases. In addition, as shown in Figure 1, emerging ship designs are employing DC voltage distribution. In such an architecture, a power conversion module containing a transformer and a rectifier converts the generator AC power into DC for distribution. The DC voltage is then manipulated into a form required by the end user (e.g. Three-phase AC, lower voltage DC, etc.).

With the continued rapid growth and development in the power electronics industry, including high-power solid-state switching devices and multi-megawatt variable speed drives, the all-electric ship with an IPS has become possible, with numerous potential advantages over a current non-IPS ship. For several years, the commercial marine industry has adopted IPS architectures with example applications including cruise liners, ferries, and icebreakers.[2] The research work proposed here will focus on one of the outstanding design challenges facing the implementation of an IPS for a surface combatant warship. Specifically, this project will focus on reducing the bus harmonics in a naval warship IPS.

The current mechanical drive system of a typical destroyer-class (DDG-51 Arleigh Burke) warship, as shown in Figure 2, requires four prime movers (gas turbines), with a combined capacity of approximately 78 MW, to drive two variable-pitch propellers via reduction gears. Ship speed control is achieved through the coordinated change of the propeller pitch and the speed of the gas turbines. Three additional engines are necessary to drive AC synchronous generators, which make available approximately 9 MW for ship service power. Thus, for most of the operating speeds of the ship, much of the installed power is “chained” to propulsion and is not available for use by electrical loads, as illustrated in Figure 2.

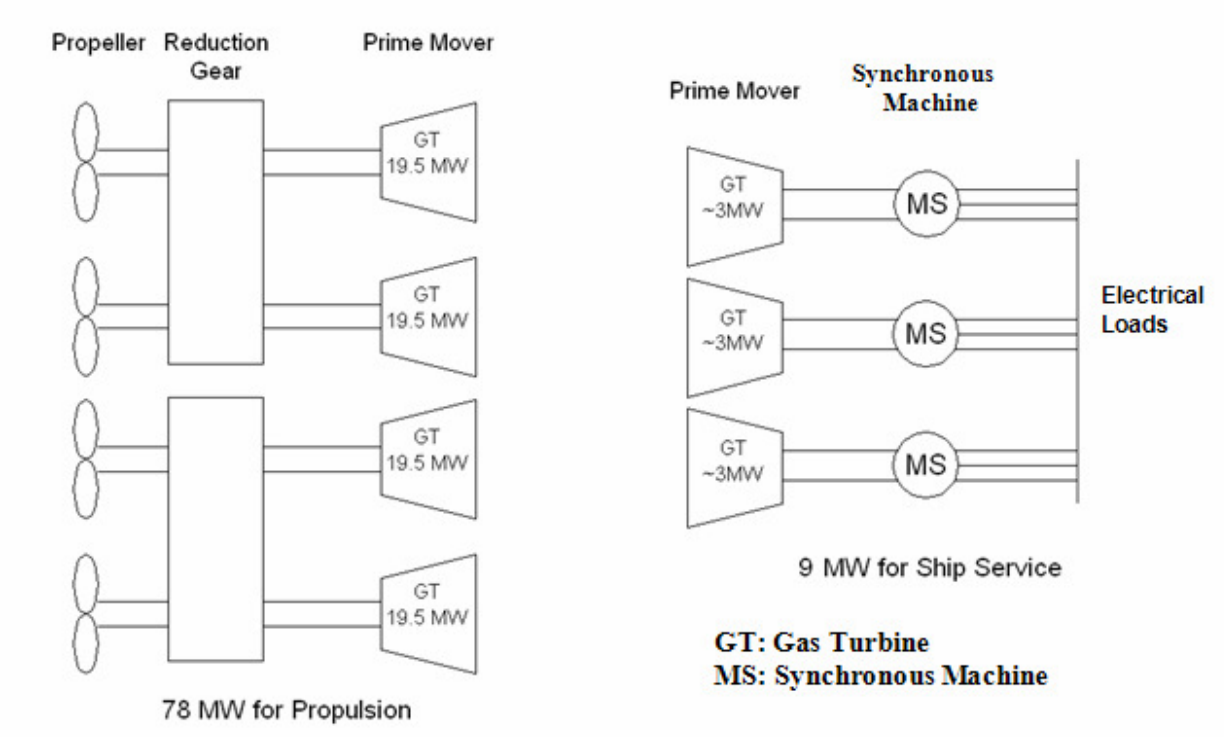

Figure 2: Current Destroyer-Class (DDG-51) Navy Ship Power System

The U.S. Navy's interest in the IPS stems primarily from its promise to increase war-fighting capability by accommodating emerging high-energy weapons. For example, rail gun technology promises to increase the land-attack range of a surface combatant while high-energy lasers or microwave weapons can figure integrally into Theater Ballistic Missile Defense (TBMD). Current surface combatant power systems do not possess the capacity to accommodate such energy-intensive weaponry. In addition, combining the propulsion and ship service electrical systems allows for the total number of engines to be reduced, for example, from seven to four, as shown in Figure 3. The number and size of these engines would be optimized for the ship mission. The proposed elimination of both reduction gear and the direct connection of the prime mover to the propeller shaft increases the acoustic performance of the ship.

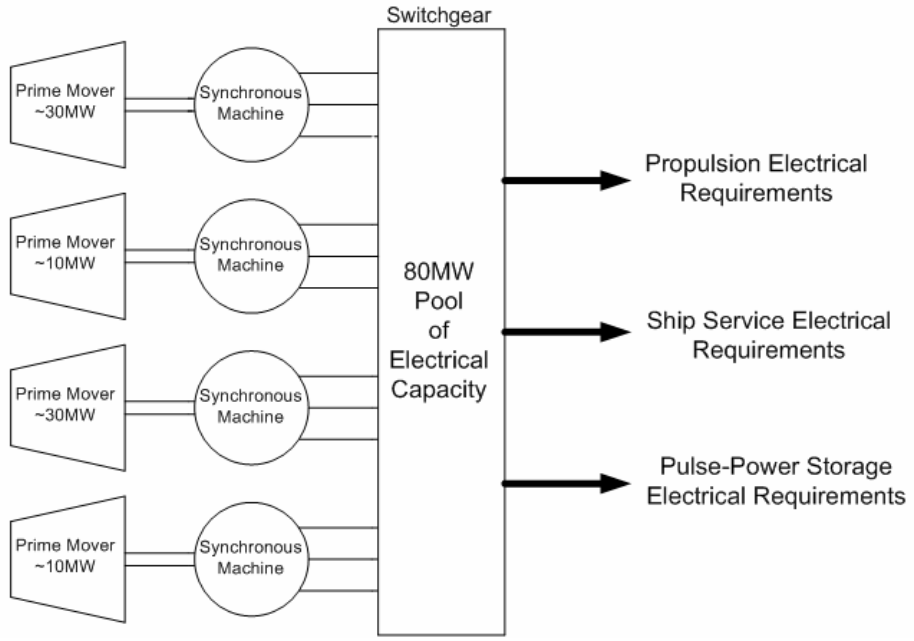

Figure 3: Notional Integrated Power System for Destroyer Class Navy Ship

In an IPS ship, the prime movers can always be run at an optimized speed while ship speed is adjusted through power electronic control of electric motors directly coupled to the propeller shaft. Thus, in spite of the lower drive-train efficiency (η), as illustrated in Figure 4, an IPS ship can always have the optimal number of prime movers operating at near their peak efficiency; hence, fuel efficiency gains can be realized.

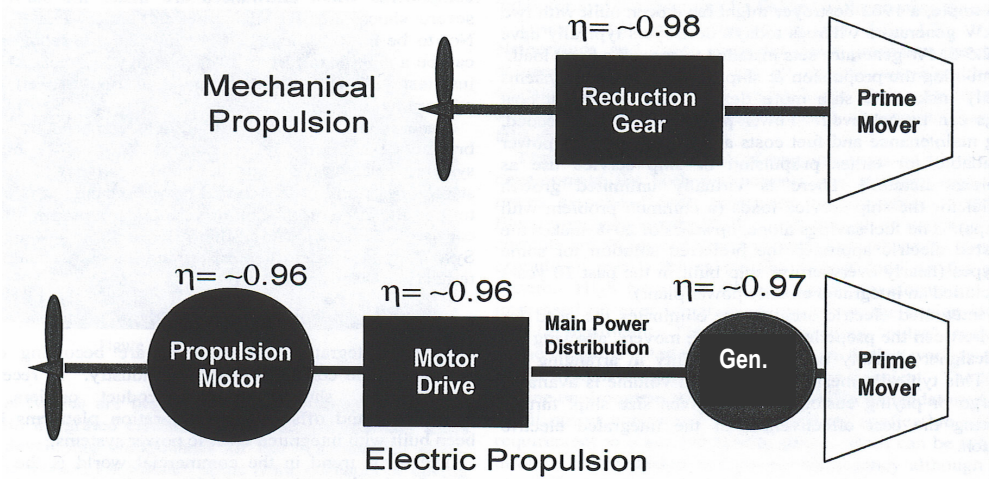

Figure 4: Electrical vs. Mechanical Propulsion[1]

The use of ship power is also made more flexible by an IPS. In the current DDG-51 class destroyer, approximately four-fifths of available power is dedicated to ship's propulsion (see Figure 2). In an IPS ship, the ship's captain has the ability to decide where to allocate his power usage. As previously stated, the new availability of electrical power for non-propulsion use is in line with the U.S. Navy's vision of future electrical weapons systems, including rail guns and high-powered microwave and laser weapons.

One of the main challenges to the IPS/all-electric ship is the introduction of significant harmonic distortion into the main distribution bus caused by the switching of non-linear power electronic equipment required by the propulsion drive and DC distribution system. The harmonic distortion has the potential to negatively impact all equipment directly connected to the main bus and may also pose Electro-Magnetic Interference (EMI) and signature concerns. As a result, these systems must be able to accommodate the harmonics generated by the power electronic converters. Hence, the generators and the power conversion equipment must either be robust enough to handle the increased harmonics or the harmonics must be decreased to an acceptable level.[1]

II. Background

A. Source of Harmonics

Harmonic currents are typically the result of non-linear loads connected to an electrical power system. In the past, only a small sector of the electrical industry has had to deal with harmonics because most loads in an electric power system were linear. However, the advent of semiconductor devices, which enable power conversion and more efficient and better control of power to loads, has resulted in non-sinusoidal load currents which then lead to non-sinusoidal bus voltages.

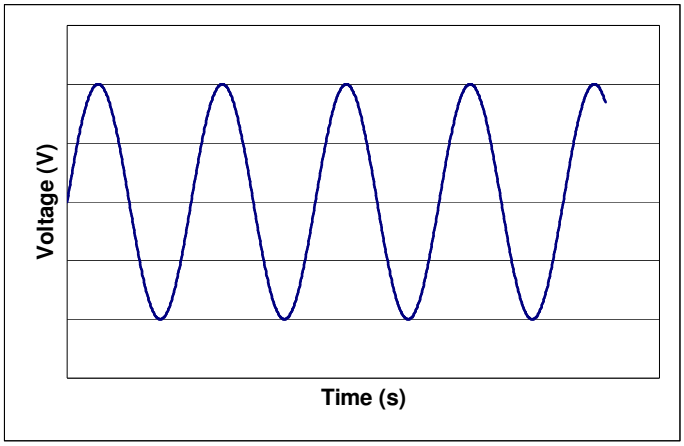

Figure 5: Sinusoidal Voltage with No Harmonics

The negative effect of harmonic currents on power systems was first noted in the late 1920's and early 1930's. As rectifiers were added to power lines and these power systems were installed and energized across the West, the harmonic currents in the power lines induced large voltages in telephone communication lines, eventually creating enough noise to interrupt telephone conversations. The problem was fixed when power companies discovered that they were able to eliminate most of the harmonic currents by using more complex rectifier topologies.[3]

Soon, with the introduction of lower-cost semiconductor devices, the country saw a proliferation of power converters throughout the power system. Components such as variable-speed motor drives and power supplies caused non-sinusoidal currents to be pulled from the power system resulting in distortion in the bus voltage. This distorted bus voltage is then distributed to loads that would prefer a perfect sinusoid. Therefore, research into ways to alleviate the impact of harmonics has become particularly important in power system design.[3,4]

The basic circuit of a six-pulse rectifier is illustrated below in Figure 6. The circuit shown in Figure 6 is called a six-pulse rectifier because its output, v_o, contains six identical pieces, as illustrated in Figure 7.

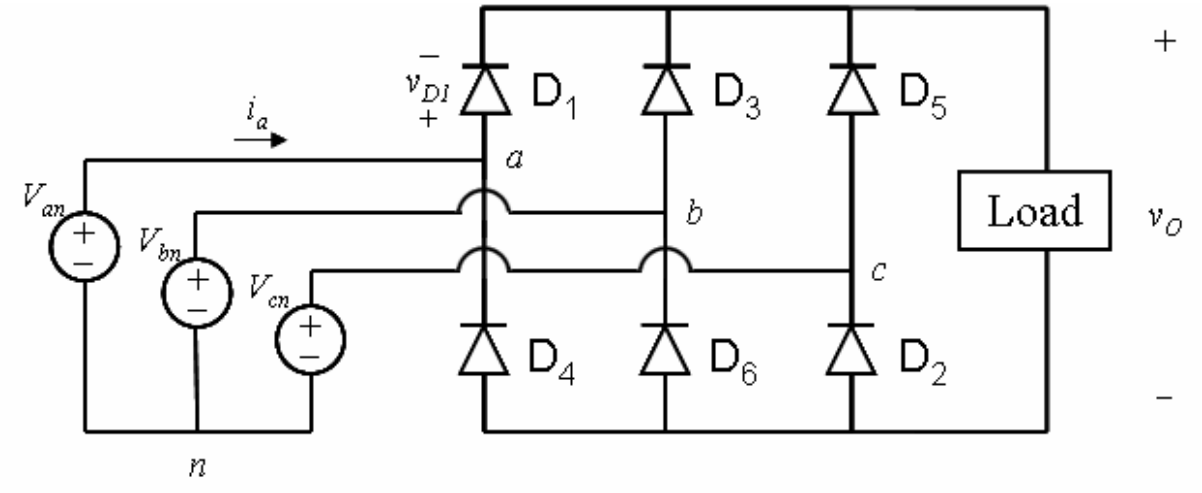

Figure 6: Six-Pulse Rectifier Circuit

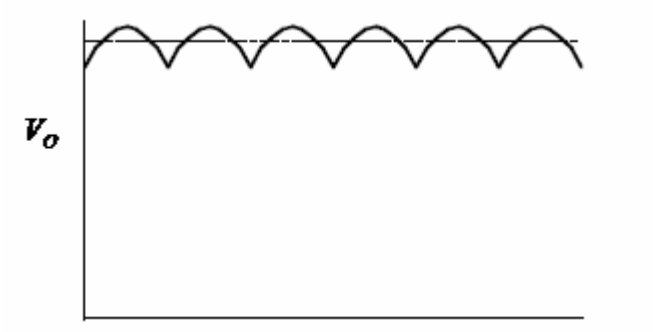

Figure 7: Output Voltage for Six-Pulse Rectifier Displaying Six Ripples for Each Cycle of Input Voltage (the dashed straight line represents the average value)

The diodes, or electronic switches, labeled from D_1 to D_6, only allow for current flow (turn ON) when there is a positive voltage across the diode. When not conducting (turn OFF), a diode serves as an open-circuit voltage blocker. As configured, the diodes will naturally turn ON and OFF in pairs due to the changing supply voltages (V_{an}, V_{bn}, V_{cn}). The pairs D_1 and D_2 are ON together, followed by D_2 and D_3, D_3 and D_4, and so on, until the cycle finishes with D_6 and D_1 conducting. For each of the six intervals, a different line voltage governs the output voltage across the load. For instance, when diodes D_1 and D_2 are ON, the output voltage is equal to the line voltage V_{ac}. Because the diodes switch ON and OFF and only one device connected to either the top or bottom rails is ON for ideal operation, the current drawn from the supply is no longer a purely sinusoidal wave and instead can appear as shown in Figure 8. The harmonics contained in this waveform are the cause of additional unwanted power losses and voltage bus distortion.

Figure 8: Representative Supply Phase Current Waveform for Six-Pulse Rectifier

B. Harmonic Analysis

A periodic waveform $f(t)$ is one that functionally satisfies

$$f(t+T) = f(t) \qquad \textbf{Equation 1}$$

where t is time and T is the period in seconds. The fundamental frequency ω in radians/second is then found from

$$\omega = \frac{2\pi}{T} \qquad \textbf{Equation 2}$$

A harmonic is defined as a component frequency of a periodic signal that is an integer multiple of the fundamental frequency. The second harmonic is a component of frequency twice that of the fundamental frequency; the third harmonic is a component of frequency three times the fundamental frequency, etc. Examples of harmonic frequencies for a 60 Hz source are illustrated in Figure 9.

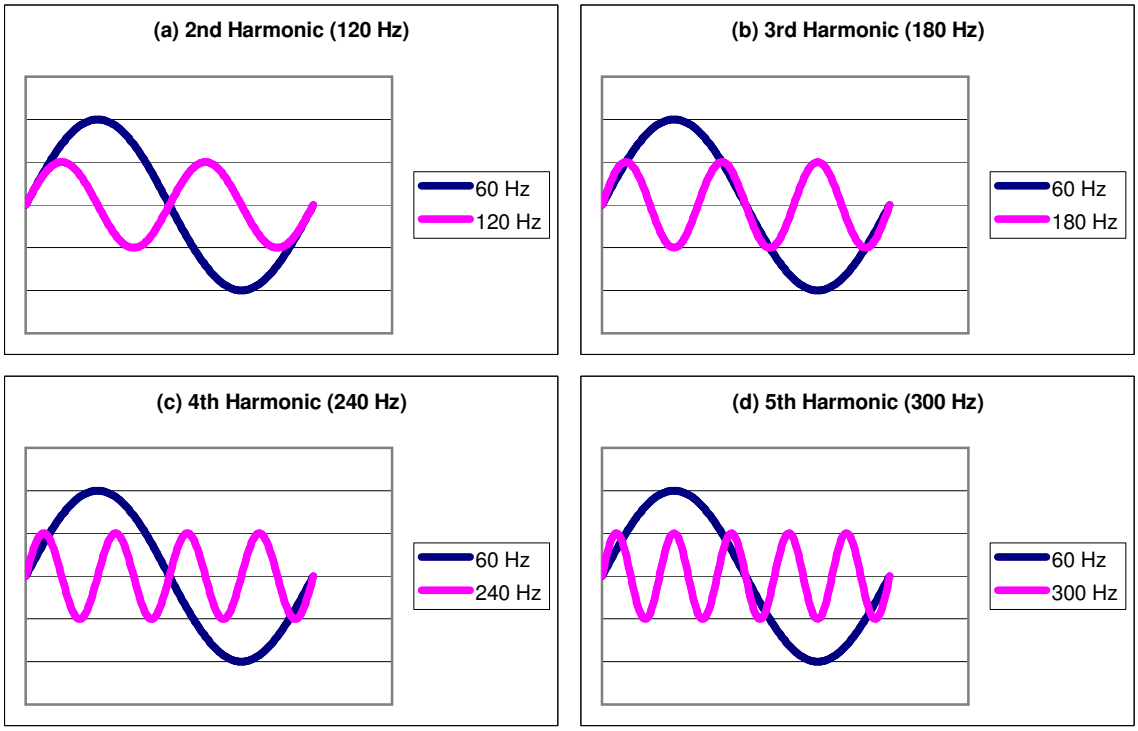

Figure 9: Fundamental Frequency of 60 Hz Sine Wave and Harmonics

The distortion due to harmonics can be studied using Fourier analysis.[5] Any periodic signal can be analyzed as a fundamental sinusoidal waveform and a set of harmonics. A pictorial example of the decomposition of a distorted periodic signal into its Fourier components is shown in Figure 10.

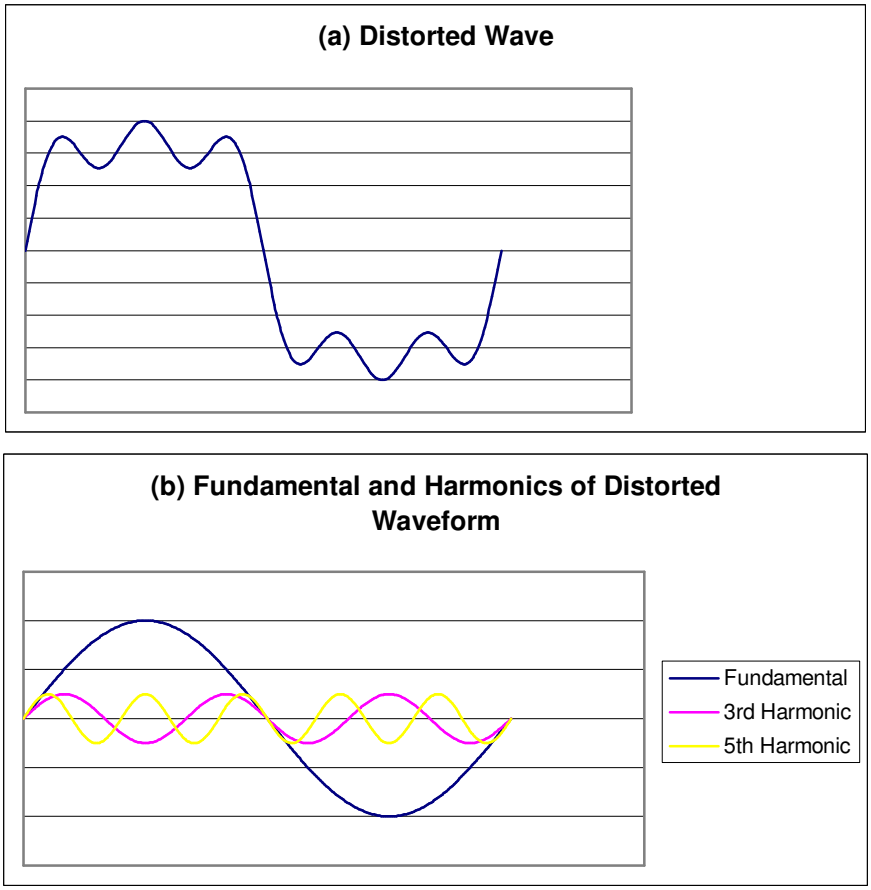

Figure 10: Decomposition of a Distorted Wave

Using Fourier analysis, any periodic waveform can be expressed using the general equation

$$f(t) = F_0 + \sum_{h=1}^{\infty} f_h(t) = \frac{1}{2}a_0 + \sum_{h=1}^{\infty}\{a_h \cos(h\omega t) + b_h \sin(h\omega t)\} \qquad \textbf{Equation 3}$$

where ω is the fundamental angular frequency expressed in Equation 2. The F_0 term is the DC or average value of the signal. In the summation, h=1 is the fundamental and each subsequent term is a harmonic.

The coefficients a_h and b_h are defined as

$$a_h = \frac{1}{\pi}\int_0^{2\pi} f(t)\cos(h\omega t)d(\omega t)$$
$$b_h = \frac{1}{\pi}\int_0^{2\pi} f(t)\sin(h\omega t)d(\omega t) \qquad \textbf{Equation 4}$$
$$h = 0,...,\infty$$

The average value F_0 is defined as

$$F_0 = \frac{1}{2}a_0 = \frac{1}{2\pi}\int_0^{2\pi} f(t)d(\omega t) = \frac{1}{T}\int_0^{T} f(t)dt \qquad \textbf{Equation 5}$$

The amount of distortion in a voltage or current waveform is quantified using the metric Total Harmonic Distortion (THD). Given a periodic current of the form

$$i_s(t) = i_{s1}(t) + \sum_{h\neq 1} i_{sh}(t) \qquad \textbf{Equation 6}$$

where $i_{s1}(t)$ is the fundamental, the distortion component of the current is found by subtracting the fundamental from the periodic signal.

$$i_{dis}(t) = i_s(t) - i_{s1}(t) = \sum_{h\neq 1} i_{sh}(t) \qquad \textbf{Equation 7}$$

In terms of root mean square (rms) values and employing Parseval's Theorem[5],

$$I_{dis} = \sqrt{I_s^{\,2} - I_{s1}^{\,2}} = \sqrt{\sum_{h\neq 1} I^2{}_{sh}} \qquad \textbf{Equation 8}$$

where I_s is established by

$$I_s = \sqrt{\frac{1}{T}\int_0^T i_s^{\,2}(t)dt} = \sqrt{I^2{}_{s1} + \sum_{h\neq 1} I^2{}_{sh}} \qquad \textbf{Equation 9}$$

The THD can now be defined as

$$\%THD_i = 100 \times \frac{I_{dis}}{I_{s1}} = 100 \times \frac{\sqrt{I_s^{\,2} - I_{s1}^{\,2}}}{I_{s1}} = 100 \times \sqrt{\sum_{h \neq 1} \left(\frac{I_{sh}}{I_{s1}}\right)^2} \qquad \textbf{Equation 10}$$

The THD of a voltage waveform can be calculated in a similar manner. A small value of THD is desirable, implying that the fundamental amplitude is large compared to the amplitudes of the harmonics. Recommended practices and requirements for THD can be found in Reference 8. For this project, the desirable THD is less than 10%.

C. Impact and Treatment of Harmonics

The impact of harmonics on power systems is found mainly in the additional losses due to heating that can cause equipment to malfunction. The result is that equipment must be derated to handle both the intended load and the additional harmonic load. If the derating is not adequate, the long-term thermal performance of the generators and transformers connected to the bus can also be compromised. Generator efficiency can be reduced by as much as 10% of that which would be experienced by a purely sinusoidal load current. Additional harmonic torque can also be developed, causing cogging (unsmooth start) or crawling (high slip) in induction motor loads. Transformers are primarily impacted by heating losses.

In addition, harmonic currents produce voltage distortion, as shown in Figure 11. Many devices are not capable of handling more than 5% voltage THD without experiencing malfunctions, including the controls devices for phase-controlled rectifiers used for DC distribution. In a U.S. Navy warship, malfunctions of key systems are clearly unacceptable.

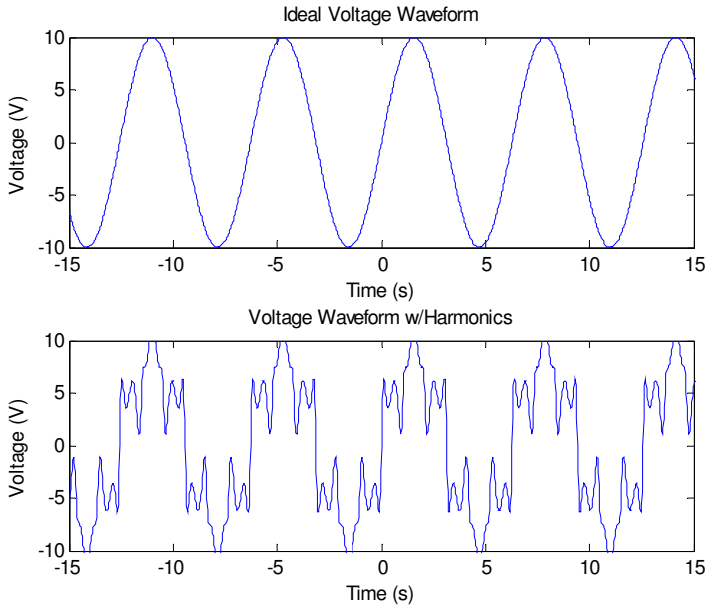

Figure 11: Severe Voltage Distortion as a Result of Harmonic Currents

There are three main approaches to improving THD and mitigating the impacts of harmonic currents. The first is the use of passive shunt filters, which are designed to absorb harmonic current, illustrated in Figure 12. The filters are designed as a series combination of inductors and capacitors that can be tuned to the desired harmonic frequency. The advantages of shunt filters include affordability, reliability, and low maintenance. The drawback is that shunt filters must be specifically designed and tuned for each application.

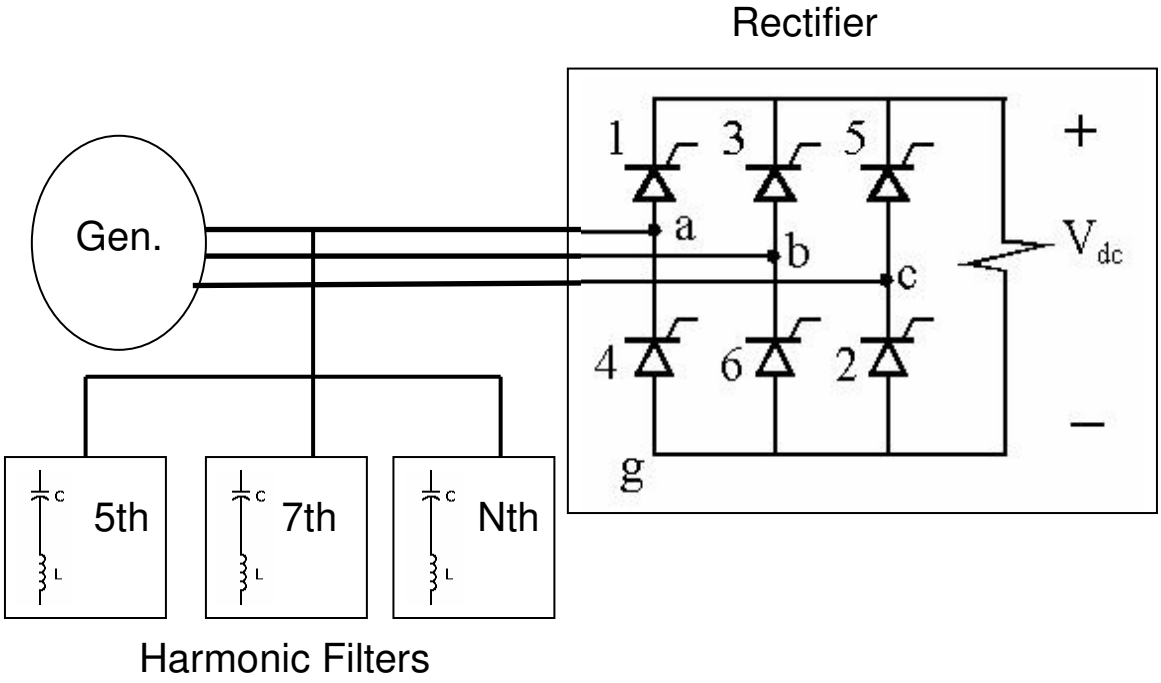

Figure 12: Implementation of Passive Filtering for a-phase for Reducing the 5th, 7th, and Nth Harmonics (same filtering would also be added for the b and c-phases)

The second approach is the use of multi-pulse rectifiers, examples being twelve-pulse, eighteen-pulse, and twenty-four-pulse rectified systems. Rectifiers that employ more than six pulses require specially designed transformers to achieve the necessary phase-shifted source voltages, as well as additional semiconductor devices. If these devices are thyristors, then they each require a snubber and gating circuit, adding circuit cost and complexity. Harmonics are reduced by phase multiplication, where the lowest harmonic present is shifted to higher frequencies, with the amount of shift dictated by the number of pulse rectifier sections. The rectifier approach has been successfully implemented, but the cost and volume issues associated with a shipboard implementation have received minimal attention in the literature.

The final method is the use of active filtering or current injection. Harmonic currents can be reduced or cancelled by injecting equivalent currents that are 180° out of phase. However,

active filtering requires additional power converters with associated controls and coordination.[1] The investigation of active filters is beyond the scope of this research effort.

The goal of this project is to compare competing strategies that seek to reduce bus harmonics in a naval warship integrated power system. The subsidiary benefit of this task is to improve the efficiency and minimize the derating factor for shipboard engines, generators, and transformers. The method of reducing harmonics is a system based on rectifiers of varying complexity and passive filtering. The candidate systems are simulated and evaluated in software, as well as constructed and validated in the laboratory at a reduced scale. The data, coupled with vendor information regarding size, weight, and acquisition costs, lead to a recommended solution.

III. Simulation

A. Six-Pulse Rectifier System

The simulation part of the project was implemented using PSCAD®, a commercially available software package used in the power system industry.[6] A six-pulse diode rectifier connected to an ideal three-phase power supply was initially modeled. The ideal six-pulse rectifier model is shown in Figure 6. After verification of the accuracy of the ideal model with theory, the complexity of the system was increased by replacing the diodes with thyristors, adding a non-ideal three-phase power supply source behind impedance, and adding snubber circuits to the thyristors. The new model, shown in Figure 13, was tested using specifications derived from the U.S. Navy's Philadelphia Land Based Engineering Site (LBES) test facility, whose parameters are shown in Table 1.

Table 1: Parameter Values for Six-Pulse Rectifier Test System

Parameter	Value
Source Frequency	60 Hz
Line to neutral Peak Voltage	3396.6 V
AC line inductance	391.7 μH
AC line resistance	1.272 mΩ
Thyristor on state voltage drop	1 V
Thyristor on state resistance	130 μΩ
Snubber capacitance	9 μF
Snubber resistance	3.33 Ω
DC link inductance	666.67 μH
DC filter capacitance	30 mF
DC link resistance	3.3 mΩ
Load resistance	4.13 Ω

Since waveform reproductions were the only available data for comparison, the accuracy of the model was verified by comparing the waveform of the A-phase of the supply current (Figure 14) with known results from both Reference 16 (Figure 15) and LBES simulations. The

LBES simulations were performed using Advanced Continuous Simulation Language (ACSL) (Figure 16) and SABRE (Figure 17) simulation programs.

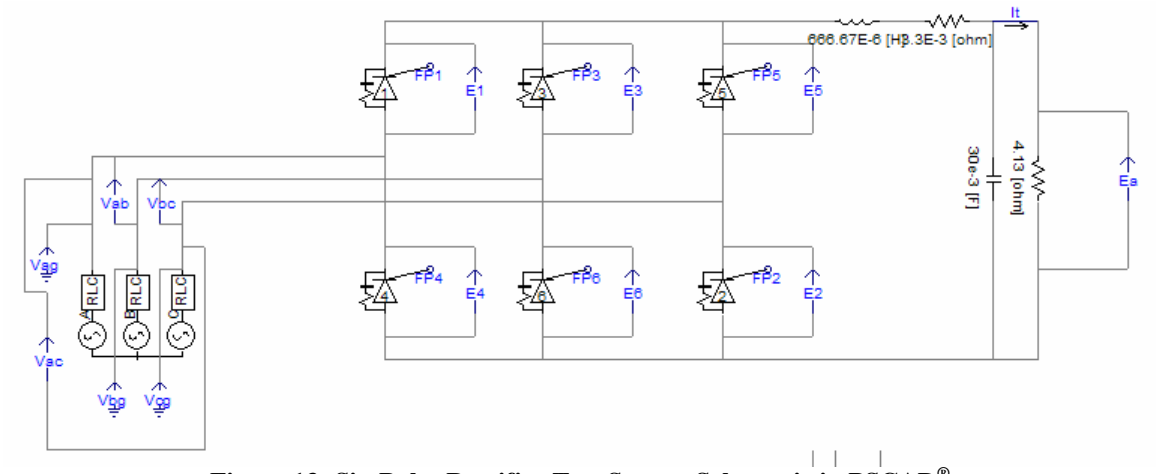

Figure 13: Six-Pulse Rectifier Test System Schematic in PSCAD®

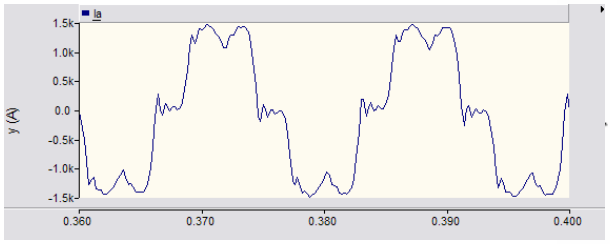

Figure 14: PSCAD® Simulation Waveform for a-phase Current from Six-Pulse Rectifier Test System

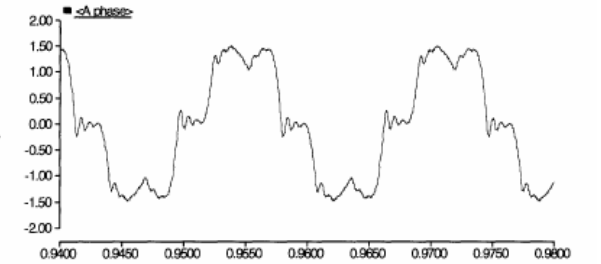

Figure 15: PSCAD® Simulation Waveform for a-phase from Reference 16[4]

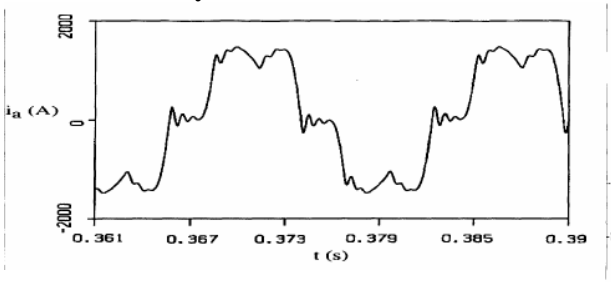

Figure 16: ACSL Simulation Waveform for a-phase Current[7]

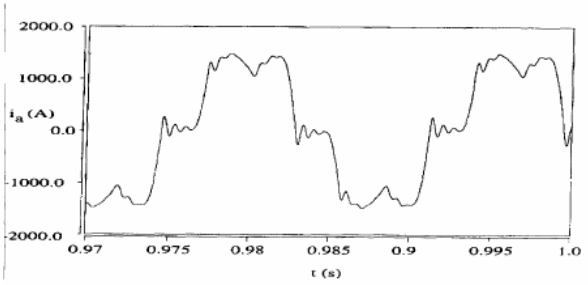

Figure 17: SABRE Simulation Waveform for a-phase Current[7]

Based on the nearly identical waveforms, we are confident in the accuracy of the six-pulse rectifier model. PSCAD® post-processing capability calculates the THD of the a-phase current as 27.5%, where this high value demonstrates the need for some harmonic mitigation strategy.

B. Thyristor Firing Control

The previous waveforms were generated using a natural line-commutated six-pulse rectifier, where the thyristors behaved as diodes. In an IPS, the propulsion motor drive rectifier and the DC distribution rectifier can be operated with a phase delay in order to control the respective DC-link voltage. Therefore, for this project, thyristor control was also implemented. Thyristors behave in the same manner as diodes but allow for greater control because the angle of turn on, or firing angle, can be set as desired. Controlling the firing angle of the thyristors for turn on allows for the control of the DC voltage output, either increasing or decreasing the amount of power delivered to the load. This control is particularly important when there is a need to interrupt the flow of power due to a fault (anomaly) on either the source or load side of the rectifier.

The thyristor controls were developed by noting that each thyristor has a unique 180° range where it is forward biased and can be gated ON. There is one line voltage that is always positive over the 180° turn ON range. For thyristor 1 in Figure 13, the coinciding line voltage is $V_{ac.}$ To identify the "in-range" condition, a comparator was used to compare the appropriate line voltage with ground, outputting a HIGH signal when in range and a LOW signal when out of range.

The initial attempt at controlling the turn-on of the thyristors utilized the cosine comparison method. For each thyristor, there is also a corresponding line-to-neutral voltage that

is single valued for the entire "in-range" condition. For thyristor 1, the appropriate line-to-neutral voltage was $-V_{bg}$. By overlaying the line-to-neutral voltage with a control voltage $V_{control}$, the thyristor can be gated ON at the point of intersection between the two signals. A second comparator was used to identify the point of intersection. The two comparator outputs were then used as the inputs to an AND logic gate, whose output (*FP1* in Figure 18) was used as the firing control for the respective thyristor. The entire firing signal control circuit for thyristor 1 is shown below in Figure 18, where nV_{bg} represents $-V_{bg.}$

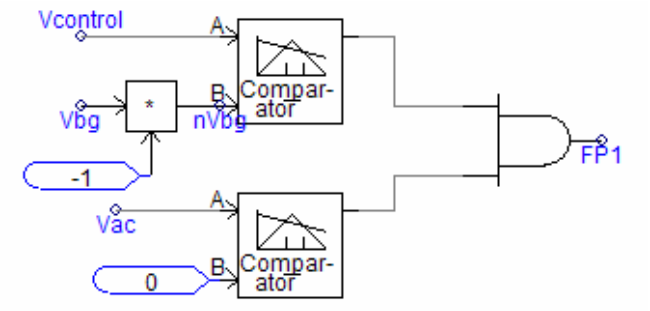

Figure 18: Firing Signal Control Circuit for Thyristor 1 of Figure 13

Due to bus voltage harmonics, this firing control circuit did not work reliably and seemed to introduce additional harmonics or limit cycles into the system. As a result, a time-delay method was developed.

The time-delay method of controlling the thyristor first identifies the "in-range" condition, as discussed previously. The firing angle was then incorporated as a time delay signal, which was implemented by knowing that the source frequency was 60Hz. The correct firing pulse signal delay time was calculated by multiplying the period of the line-to-neutral voltage by the fraction of the angle to 360° times the period of the function, as shown in Equation 11.

$$FP = \frac{1}{60Hz} * \frac{FA}{360°} \qquad \textbf{Equation 11}$$

Figure 19 shows the implementation of the time-delay method for control of thyristor 1 (in Figure 13) in PSCAD®. Control of the remaining thyristors occurred in a similar fashion, with each thyristor's "in-range" condition first being identified and then delaying the firing pulse signal according to the desired firing angle.

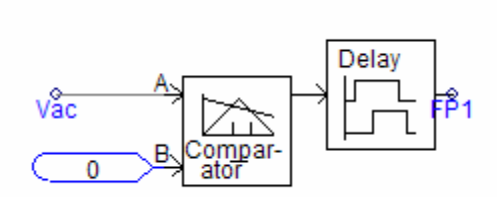

Figure 19: Time-Delay Method of Firing Control.

C. Twelve-Pulse Rectifier System

A twelve-pulse thyristor controlled rectifier model was created. The twelve-pulse rectifier is essentially two series-connected six-pulse rectifiers connected to the main bus through three-phase transformers. A representative twelve-pulse rectifier is shown in Figure 20.

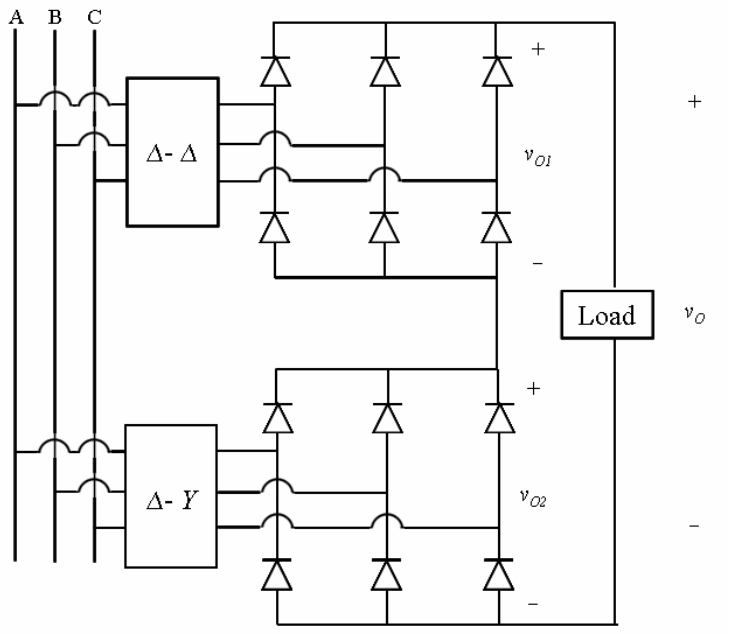

Figure 20: Twelve-Pulse Rectifier System

The addition of transformers is necessary to phase shift the source voltages so that there are in effect six phases, where one balanced set is shifted 30° from the other by the Δ-Y transformer. The model in Figure 20 shows Y-Y and Y-Δ transformers; however, the U.S. Navy intends to use Δ-Y and Δ-Δ transformers, to avoid nonlinearities introduced by a Y-Y connection. The circuit schematic of the twelve-pulse rectifier model in PSCAD® is illustrated in Figure 21.

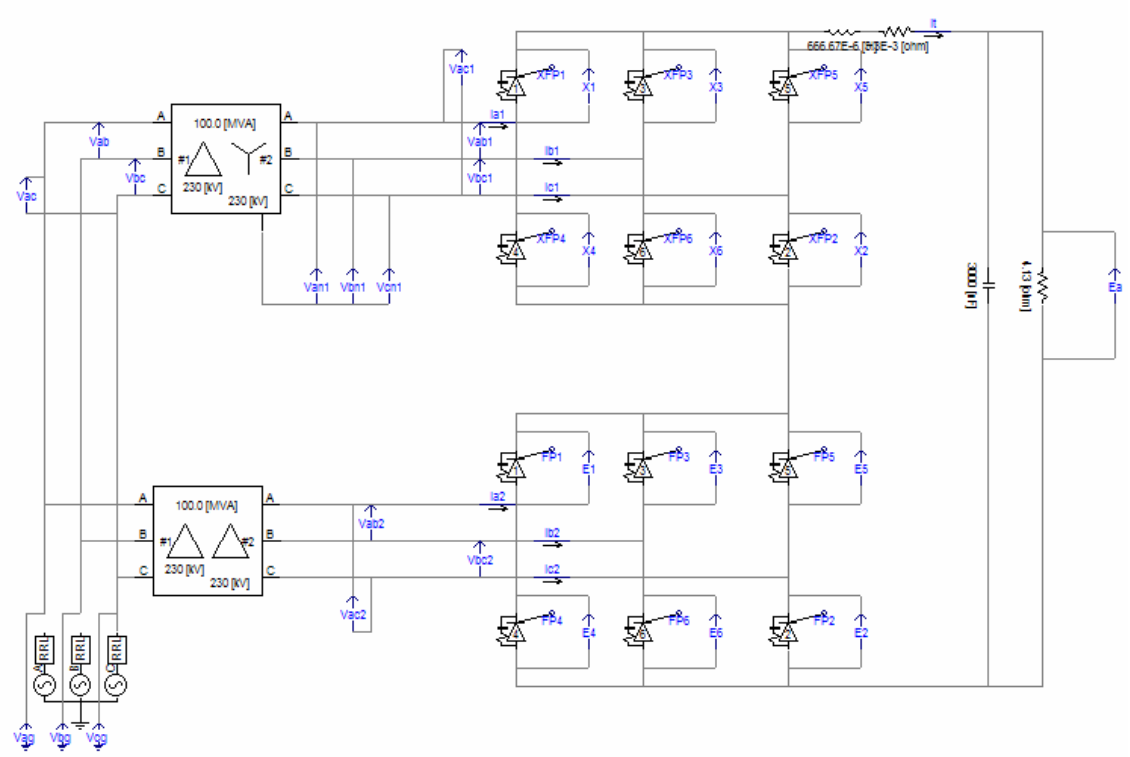

Figure 21: Twelve-Pulse Rectifier Test System Schematic in PSCAD®

There were several problems encountered when developing the twelve-pulse model. The addition of the transformers caused the output voltage on the secondary side to drop to very low levels, which was unexpected for a properly operating transformer with a 1:1 turns ratio. The simulation was also unable to extract the line-to-neutral voltage V_{an1} from the secondary side of the Δ-Y transformer. The line-to-neutral voltages are necessary to properly implement the cosine comparison method of generating firing controls for the thyristors in the top rectifier.

Through discussions with PSCAD® technical support, the transformer voltage drop was resolved by lowering the per-unit (PU) impedance of the transformer from 0.1 to 0.001. Previously, the large PU impedance value of the transformers was causing an excessively large voltage drop across the transformer impedance instead of the load impedance. By modifying the PU impedance, all line-to-neutral voltages can also now be extracted.

The additional six-pulse rectifier significantly improves the harmonic distortion in the source current. As shown in Figure 22 , the a-phase current of the source using the twelve-pulse rectifier contains fewer harmonics than the a-phase current from the six-pulse rectifier, shown previously in Figure 14.

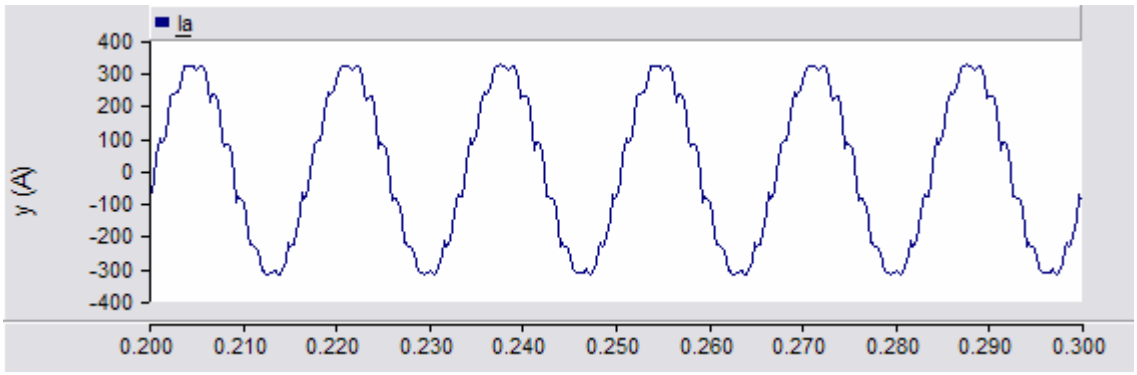

Figure 22: PSCAD® Simulation Waveform for a-phase Current from Twelve-Pulse Rectifier Test System

The results confirm what is expected from theory. The a-phase current THD is 8.92%, which is a significant improvement over the current THD of the six-pulse rectifier, which was 27.5%. However, the THD can be reduced further by the application of filtering.

D. Filtering

Passive filtering can be implemented through harmonic trap filters, containing banks of capacitors and inductors tuned to absorb the unwanted harmonics. Figure 23 demonstrates the six-pulse test system with filtering tuned to the 5th harmonic, with capacitance and inductance values derived from LBES data.

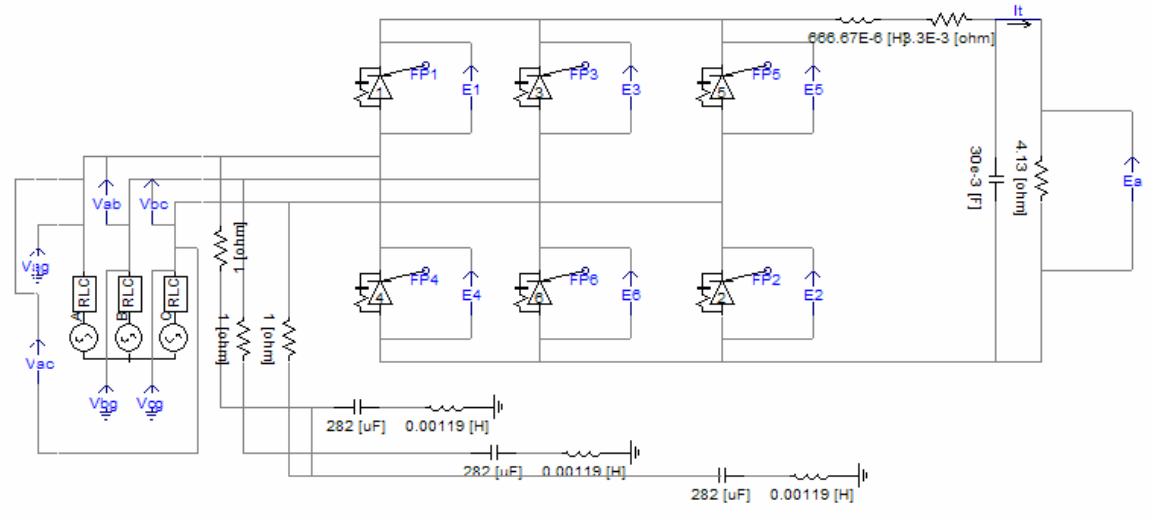

Figure 23: Shunt Filtering for Reducing the 5th Harmonic

Tuning the banks to a specific frequency can be achieved by setting the resonant frequency of the LC filter equal to the harmonic, giving the harmonic current a lower impedance path in which to travel through. In Equation 12, ω, the frequency in rad/s, is related to f, the frequency in hertz in the following manner.

$$\omega = 2\pi f \qquad \textbf{Equation 12}$$

A filter can be tuned to any harmonic $n\omega_o$, where ω_o is the fundamental frequency and n is the harmonic number through the equation

$$n\omega_o = \frac{1}{\sqrt{L_n C_n}} \qquad \textbf{Equation 13}$$

where C_n is the capacitance and L_n is the inductance.

Traditional methods of designing filtering are based on power factor correction.[8] On a terrestrial power system, the load can be assumed to be relatively constant and the filter can be designed with a capacitance that will change the power factor from lagging to near unity. For an IPS system with DC distribution, each load will have a rectifier between it and the main generation bus. The controlled rectifier load means that the displacement power factor will vary with firing angle. As a consequence, variable power factor correction is required. Therefore, a new paradigm for filter synthesis is required for shipboard systems.

While the power factor correction method is a good starting point, there remain issues with choosing the value of the capacitance. Too large of a capacitance will cause the power factor to change to leading and negate the benefits of harmonic filtering because of the additional reactive power requirement. The capacitance value must also be selected so that it does not resonate with the inductance of the generator, causing large overvoltages.

The filtering for this project was designed through simulation. Focusing on the 5^{th} harmonic filter, the simulations of the filter started with the LBES value for inductance (1.19mH, rounded to 1.2mH). The filter inductance was then varied by a factor of ten up and down from the LBES value. The corresponding matching capacitance for every value of inductance was calculated, as shown in Equation 13, to tune the filter to the 5^{th} harmonic. For each simulation run, the generator current THD as well as the actual generator current were monitored as metrics for determining the optimal value of inductance and capacitance. While an increase of several magnitudes in the generator current is expected due to the reactive power demanded by the capacitor, a smaller current is more desirable because it signifies less total power output from the generator.

The simulation runs utilized the six-pulse rectifier test system with LBES parameters, a firing angle of 0°, and using an input voltage of 100V for convenience. The data in Table 2 shows the various values of inductance that were simulated, as well as their corresponding capacitance for a tuned 5^{th} harmonic filter. The data shows a significant increase in generator current for filters with inductance values less than 1mH when compared to the generator current without filtering. Filters with inductance values greater than 1.2mH were less effective at reducing current harmonics, as demonstrated by the corresponding larger THD values. As a result, the inductance value of 1mH was selected for use in the LC filters. The value of 1mH was used for LC filters was used for the design of all harmonic filters used in this project (5^{th}, 7^{th}, 11^{th}) for cost-control and simplicity.

Table 2: LC Design

Inductance (H)	Capacitance (F)	Input Voltage (V)	Generator Current (A)	THD of Gen. Current (%)
0	0	100	2.37	29.35
0.0005	0.000562	100	18.1	4.1
0.0009	0.000312	100	10.6	7.2
0.001	0.000281	100	8.6	8.7
0.0012	0.000234	100	8.5	9.65
0.0015	0.000187	100	7.2	11.64
0.002	0.000140	100	6.8	14.6

This analysis assumes that the original rectifier system operates at near unity power factor and thus seeks a compromise between THD and operation at a leading power factor. If the rectifier is operated with phase delay, then the designer has another degree of freedom. In addition, if the filter can be built with step increments of capacitance, then that would further enable “tuning” of the system.

Table 3 shows the results of applying filtering to the twelve-pulse test system using LBES parameters. The input voltage was set at the U.S. Navy’s design of 4160V and the DC

resistive load was set to give an output voltage of approximately 1000V, which is the desired output voltage for ship-service distribution. The U.S. Navy will also operate the converters on the IPS at an as of yet undetermined firing angle. Because of this, the affect of varying the firing angle is also shown. For instance, towards the end of this project, it was learned that the DDG-1000 propulsion device utilize firing angles ranging from 0° (full power) to 45° (low speed).

Table 3: Twelve-Pulse Test System: Output Voltage, Generator RMS Current, and Generator Current THD for Various Filtering and Firing Angles

Firing Angle (°)	Filtering	V_{out} (V)	I_a RMS (A)	THD (%)
0	None	1113	42.105	14.37
0	5th	1112	261.8	2.26
0	5th+7th	1113	394.8	1.51
0	5+7th+11th	1114	446.6	1.3
0	5th+11th	1112	321.3	1.84
21.6	None	1034	40.6	15.9
21.6	5th	1034	252	2.43
21.6	5th+7th	1033	378	1.61
21.6	5+7th+11th	1035	435.4	1.34
21.6	5th+11th	1034	304.5	1.93
45	None	808	34.72	21.5
45	5th	808	238	2.6
45	5th+7th	809	369.6	1.7
45	5+7th+11th	808	422.8	1.42
45	5th+11th	808	289.8	2.06

The data demonstrates the reduction of harmonics in the generator current through the addition of filtering. The increase of the generator current due to filtering can also clearly be seen. Although the harmonic trap filter tuned to the 5^{th}, 7^{th}, and 11^{th} harmonics resulted in the lowest THD values, it also created a ten-fold increase in generator current. The system of harmonic filters tuned to the 5^{th} and 11^{th} may be the best balance of reducing THD while limiting the increase in generator current. This could be due to the fact that the 5^{th} harmonic filter may be

able to eliminate some of the 7^{th} harmonic, while the 11^{th} harmonic filter can eliminate some of the 13^{th} harmonic.

From the data, an increase in the firing angle of the thyristor also causes an increase in the THD. This is due to the introduction of more harmonics as a result of delaying the turn-on of the thyristors. However, despite the increase in harmonics, the harmonic filters are still able to effectively reduce the THD value. Future research could revisit the idea of selecting the filter capacitance to achieve a certain power factor value. The required inductance is then found from Equation 13. To account for changes in operating conditions, the amount of power factor correction could be made incremental.

E. Full Integrated Power System

The goal of the project was to assess the rectifier choice and filter design for a shipboard IPS. With that in mind, a representative integrated system was selected, guided by vendor-supplied data. The system consists of a twelve-pulse thyristor rectifier for ship service DC distribution, a twelve-pulse diode rectifier for pulsed power and radar loads, and a six-pulse thyristor rectifier for ship propulsion. The system is shown in Figure 24.

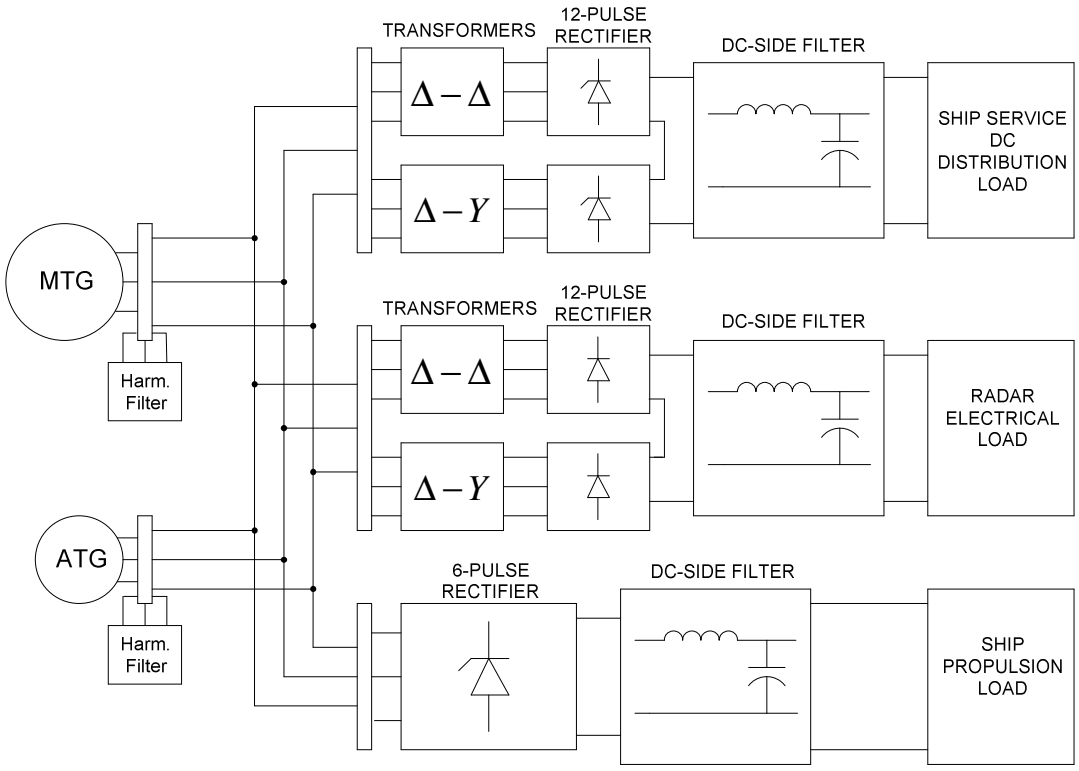

Figure 24: Full-Integrated Power System Model

For the DDG-1000, the U.S. Navy is using a 4160V input voltage to the rectifier systems. The DC voltage output of the Ship Service load will be 1000V with a full-power output of approximately 3MW. The propulsion load will utilize a full-power 5600V DC voltage and the power will range from 0 to 34MW of power per propeller. The pulsed-power and radar loads will

receive an assumed 5600V DC output voltage with a peak power of 5.8MW of power. This arrangement assumes two such systems to account for two propeller shafts and redundant loads. The MTG stands for main turbine generator, while ATG stands for auxiliary turbine generator.

Figure 25 shows the full integrated power system schematic as modeled in PSCAD®. An aggregate machine model was used to represent both the MTG and ATG. The aggregate model consisted of a voltage source behind a sub-transient reactance as was used in prior efforts [16]. In future research, the impact of separate sources can be addressed. This would enable the investigation of the influence of the individual sub-transient reactance values.

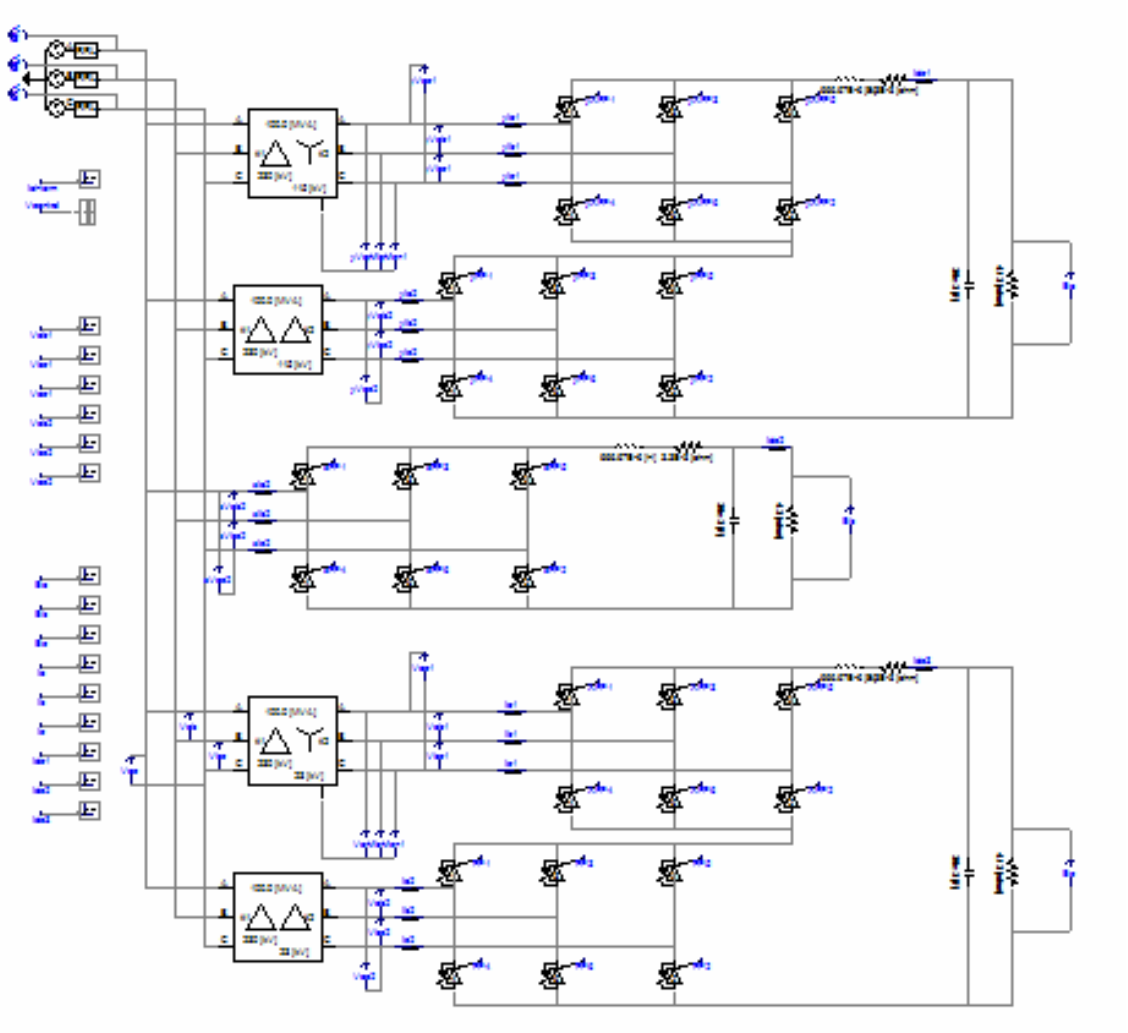

Figure 25: Full Integrated Power System Schematic in PSCAD®

Table 4 shows the results of the PSCAD® simulation of the full integrated power system with various harmonic filters and various propulsion loads. For these simulations, all converter systems were operated with a 0° firing angle. In the table, the subscript *a* represents the pulsed power and radar load, the subscript *b* represents the propulsion load, and the subscript *c* represents the ship service distribution load, where E_a is the DC output voltage for the *a* load and R_a is the resistive load for *a*.

Table 4: Full Integrated Power System: Supply Current THD, Output Voltage, and Power for Various Filtering and Propulsion Loads

Filtering	THD	E_a (V)	R_a (Ω)	$Pout_a$ (W)	E_b (V)	R_b (Ω)	$Pout_b$ (W)	E_c (V)	R_c (Ω)	$Pout_c$ (W)
none	16.95	5600	22	1425455	5640	4.13	7702082	1030	0.32	3315313
5	8.096	5360	22	1305891	5400	4.13	7060533	971.5	0.32	2949413
5+7	3.16	5473	22	1361533	5515	4.13	7364461	982	0.32	3013513
5+7+11	1.48	5524	22	1387026	5563	4.13	7493213	990	0.32	3062813
5+7+11+13	1.23	5546	22	1398096	5591	4.13	7568833	994	0.32	3087613
none	20.4	5590	22	1420368	5600	2.13	14723005	1000	0.32	3125000
5	3.95	5314	22	1283573	5324	2.13	13307500	956	0.32	2856050
5+7	2.95	5377	22	1314188	5384	2.13	13609134	965	0.32	2910078
5+7+11	1.45	5432	22	1341210	5447	2.13	13929488	976	0.32	2976800
5+7+11+13	1.25	5454	22	1352096	5470	2.13	14047371	979	0.32	2995128
none	23.7	5590	22	1420368	5550	1.13	27258850	1000	0.32	3125000
5	3.66	5114	22	1188773	5074	1.13	22783607	922	0.32	2656513
5+7	2.51	5179	22	1219184	5138	1.13	23361986	932	0.32	2714450
5+7+11	1.38	5244	22	1249979	5216	1.13	24076687	943	0.32	2778903
5+7+11+13	1.23	5267	22	1260968	5230	1.13	24206106	947	0.32	2802528
none	25.1	5590	22	1420368	5520	0.8	38088000	1030	0.32	3315313
5	3.46	4904	22	1093146	4824	0.8	29088720	888	0.32	2464200
5+7	2.74	5000	22	1136364	4920	0.8	30258000	901	0.32	2536878
5+7+11	1.31	5058	22	1162880	4986	0.8	31075245	912	0.32	2599200
5+7+11+13	1.15	5081	22	1173480	5018	0.8	31475405	915	0.32	2616328

The decrease in the DC output voltage is a result of holding the voltage in the voltage-behind-reactance source fixed at 4160V. Ideally, a feedback control system would control the input voltage to keep the output voltages at the desired levels.

The data again demonstrates that the addition of filtering has a significant impact of reducing generator current THD. Adding more filters tuned to the appropriate frequencies increases the capability of the filtering to reduce THD. However, the reduction in THD still causes an increase in the reactive power supplied by the generator due to the choice of capacitor value, forcing the generator to supply a larger total power.

IV. Hardware

The goals of the hardware investigations are to further validate simulation results, demonstrate the efficacy of filtering, and to explore real-world component effects.

A. Six-Pulse Rectifier System

Laboratory hardware testing involved three parts: design and building of the rectifier system, collecting and importing data into MATLAB®, and using MATLAB® to calculate THD. A six-pulse thyristor rectifier system was constructed using Lab-Volt® modules. For initial tests, the system contains a three-phase variable (0-120 V_{rms} line-to-neutral, 5 A) power supply (module #8821-20) connected to a six-pulse thyristor rectifier (module #8841-20), shown in Figure 26. Firing control was directly implemented through a Lab-Volt® firing control module (module #9030-30) that was synchronized to the supply voltages. The load consisted of a large DC link inductance of 0.8H (module #8325-10), a large DC link capacitance of 2500µF (module #8837-00), and a variable resistance resistive load (module #8311-00) set to 57.15Ω.

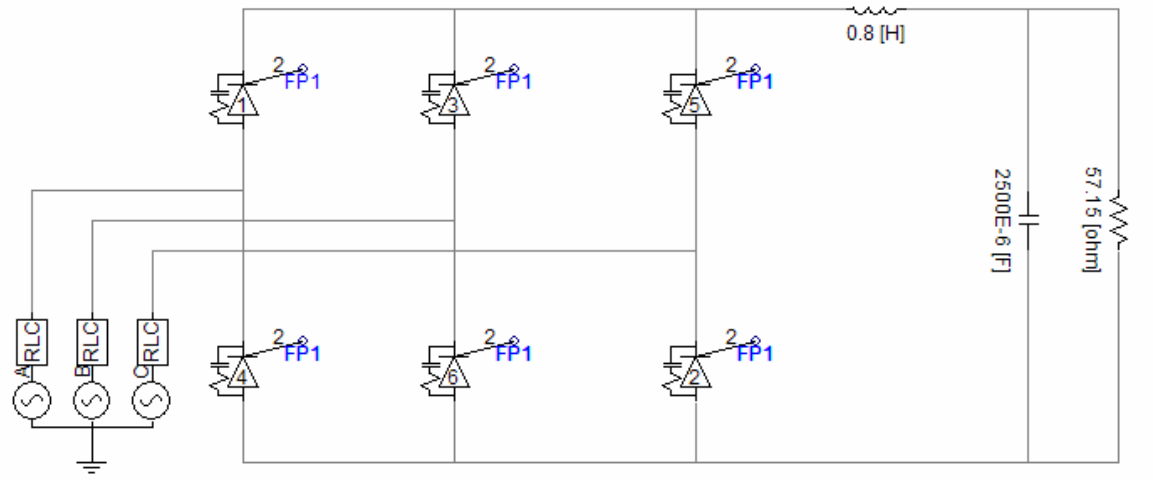

Figure 26: Six-Pulse Thyristor Rectifier Circuit Implemented using Lab-Volt® modules

Using a Tektronix A622 current probe, one of the supply phase currents was displayed on a Tektronix TDS2024 oscilloscope. Through a GPIB board, the waveform appearing on the oscilloscope was then imported into MATLAB®. The GPIB interface was capable of exporting a maximum of 2500 data points from the waveform into MATLAB®.

In MATLAB®, the Fast Fourier Transform (FFT) was performed on the data to extract frequency data. The THD is then calculated. A MATLAB® script, documented in Appendix A, was written to automatically extract the waveform, perform the FFT, and calculate the THD. The script was validated through testing of waveforms in which the THD can be easily calculated, such as $5\cos(w_0 * t) + 2\cos(5w_0 * t) + \cos(7w_0 * t) + ... +$.

B. Windowing

Because the FFT performs a Fourier Transform at discrete times over a finite interval of time, the phenomenon known as leakage is introduced. Leakage results in a distortion of the frequency data, introducing large side lobes and returning values for harmonics that are not present in the waveform, as shown below in Figure 27.

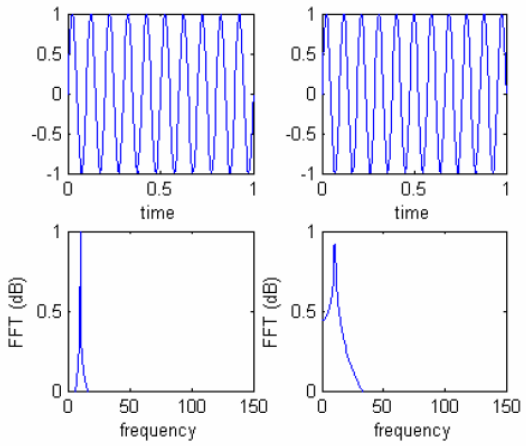

Figure 27: Expected FFT versus Leakage Effects[9]
(a) FFT of a Perfectly Periodic Waveform
(b) FFT of a Waveform Displaying Leakage

Applying a window forces the beginning and end of a waveform to zero, resulting in a perfectly periodic function with no abrupt transitions. The result is greatly reduced side lobes and better frequency resolution, as shown in Figure 28.

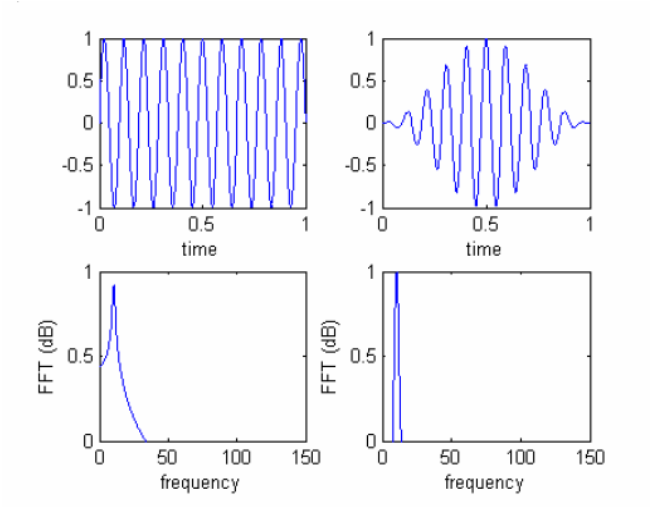

Figure 28: Leakage Effects versus Windowing[9]
(a) **FFT of a Waveform Displaying leakage, No Window Applied**
(b) **FFT of a Waveform with Hanning Window Applied**

The MATLAB® script contains a number of different windows, including Flat-top, Hanning, Hamming, or Blackman, that could be applied to the data for better frequency resolution. The Hanning and Hamming windows give the best frequency resolution, while the Blackman window has excellent amplitude accuracy.

THD data for one phase of the supply current for each of the windows is shown in Table 5. The data includes THD values at firing angles of 0° and 20.4°.

Table 5: THD Data for Various Windows and Firing Angles

Window Type	**THD Value (%)**	
	0° Firing Angle	*20.4° Firing Angle*
Rectangular (No window)	28.51	30.76
Hanning	28.46	30.82
Hamming	28.64	30.81
Blackman	28.45	30.86

The figures below are sample waveforms generated by the MATLAB® script demonstrating the use of windowing. In Figure 29, the waveform for one phase of the supply current for a thyristor firing angle of 20.4° is shown in the top half of the figure. The effect of applying a Hanning window is shown in the bottom half of the figure.

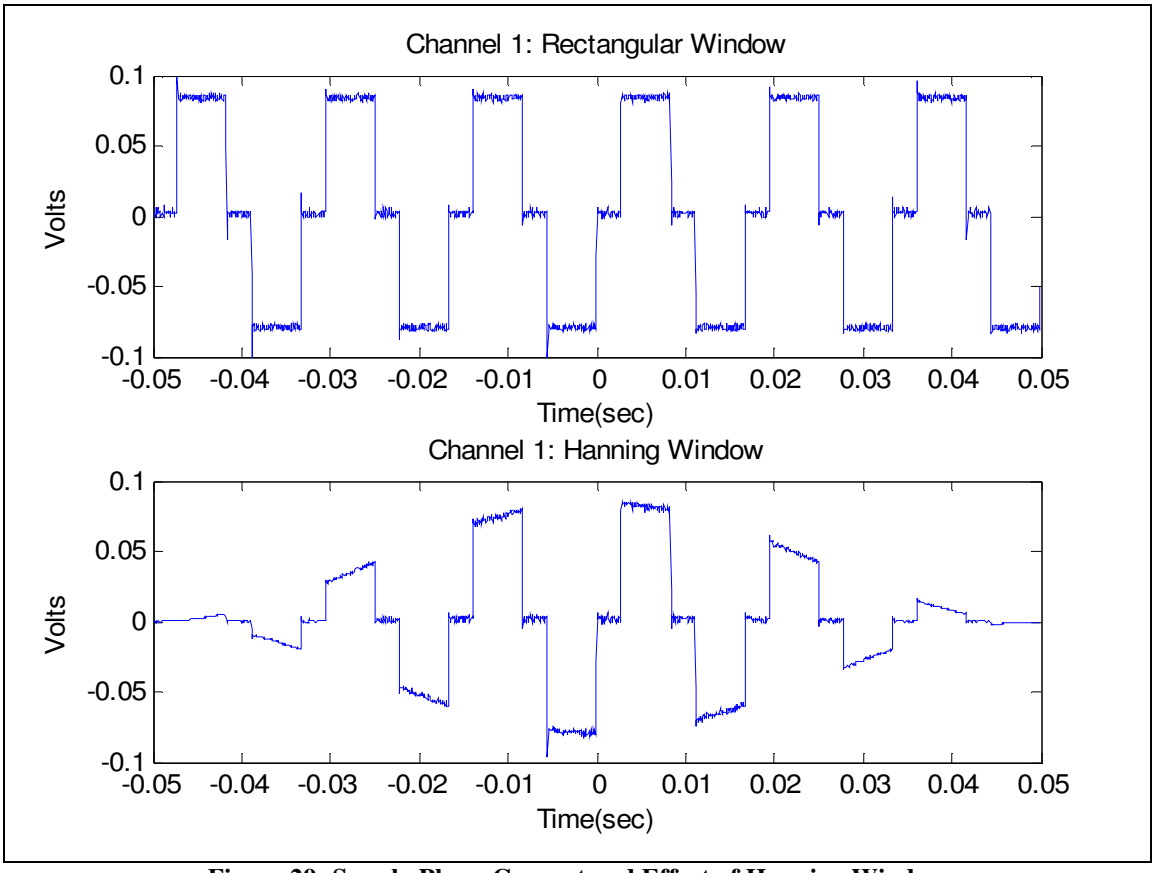

Figure 29: Supply Phase Current and Effect of Hanning Window

Figure 30 shows the FFT of the waveforms above. The FFT of the waveform with the Hanning window has considerably better frequency resolution than the FFT of the rectangular window.

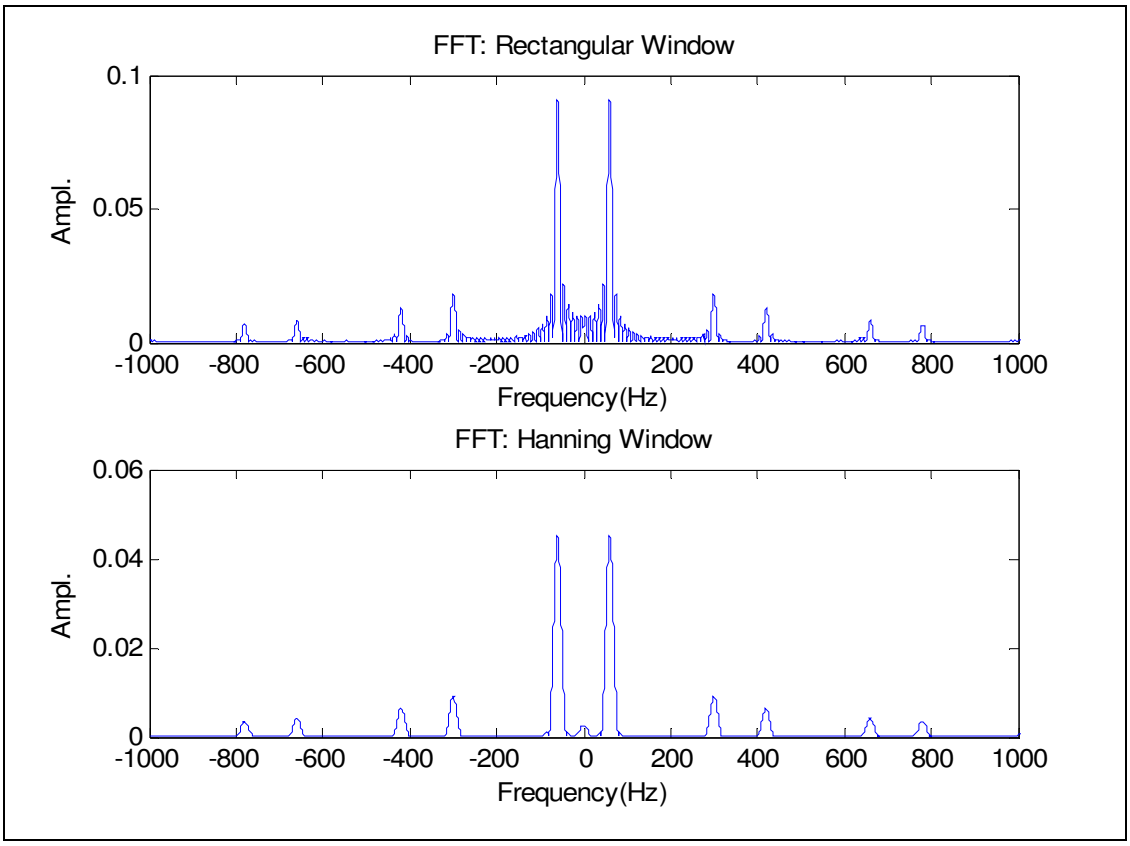

Figure 30: FFT of Supply Phase Current and Effect of Hanning Window

C. Twelve-Pulse Rectifier System

With the ability to extract waveforms from the six-pulse hardware model with thyristor control, the twelve-pulse diode rectifier was constructed using two six-pulse systems, a set of transformers (module #8341-00), and diodes (module #8842-10) instead of thyristors. The load again consisted of a large DC link inductance of 0.8H and a large DC link capacitance of 2500μF. The resistive load was increased to 300Ω to decrease the required current and increase the measurable output voltage.

For input power, a synchronous motor (module #8241-00) was used to drive a synchronous generator (module #8241-00), which created the three-phase output voltages. The

field winding of the generator was supplied from a variable DC voltage source to enable some adjustment of the output voltage. The transformers were characterized using standard tests, including a DC test, short-circuit test, and open-circuit test. The twelve-pulse test system is represented by the model shown in Figure 31.

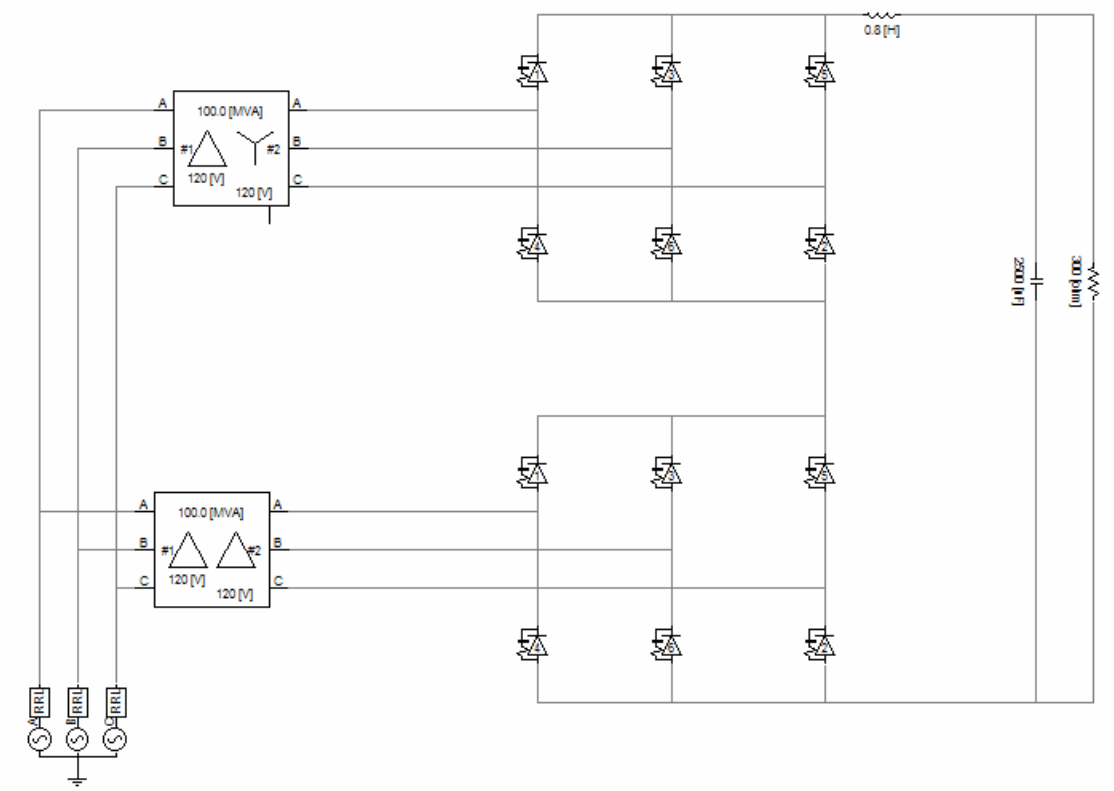

Figure 31: Twelve-Pulse Diode Rectifier Model Implemented Using Lab-Volt®

The actual hardware setup of the twelve-pulse system is shown in Figure 32. By slightly modifying the wiring connections, the twelve-pulse rectifier system can be operated as a six-pulse system. In Figure 32, the modules on the bench on the left are the transformers and power diodes. The top section of the cart contains the modules for the DC load, as well as the power thyristors and thyristor control module. The bottom section of the cart contains the power supply, motor, and generator.

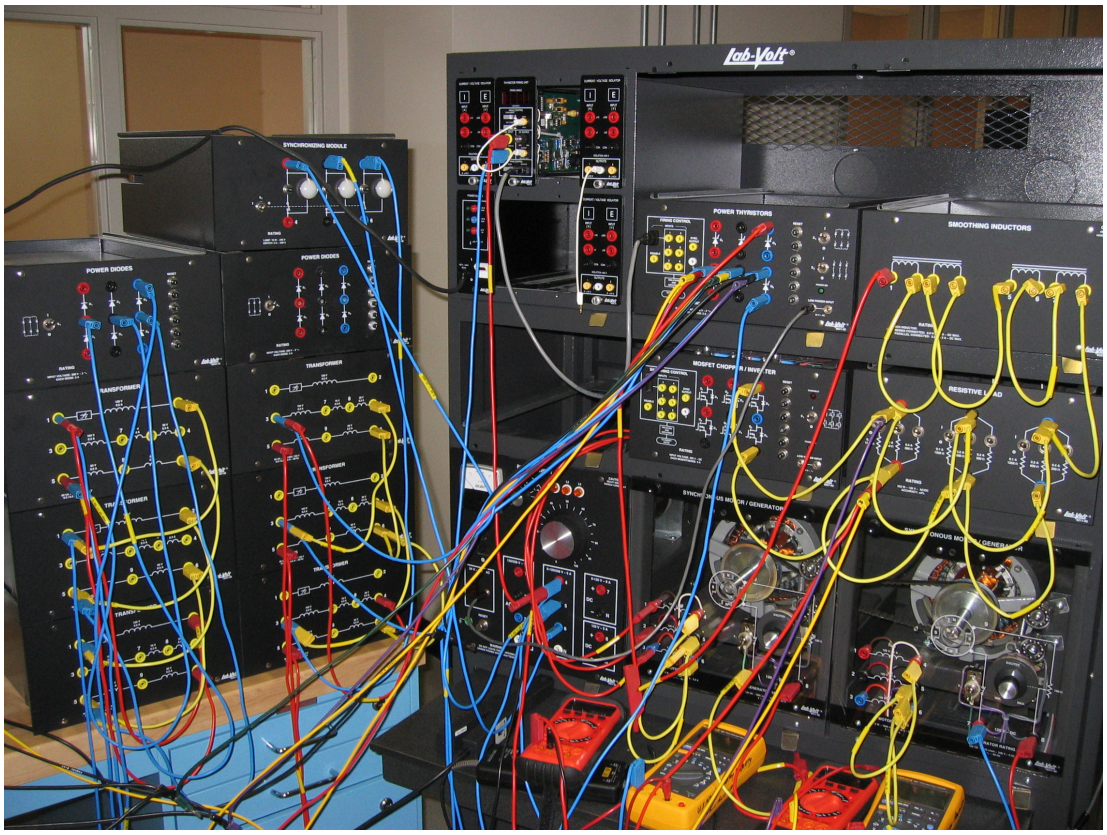

Figure 32: Hardware Setup of Multi-Pulse Converters

Despite decreasing the attached load, there was still a large voltage drop when comparing the measured output voltage to the input voltage. Ideally, a twelve-pulse converter should double the output voltage when compared to six-pulse converter; however, our system had a maximum output voltage of around 13V with an input of 50V, when the system reached a maximum load current.

The system was still able to extract the generator current data to calculate THD. Figure 33 shows one phase of the supply current, with a calculated THD of 9.25%. The THD result is similar to the results obtained from simulation (THD of 8.97%, as discussed previously).

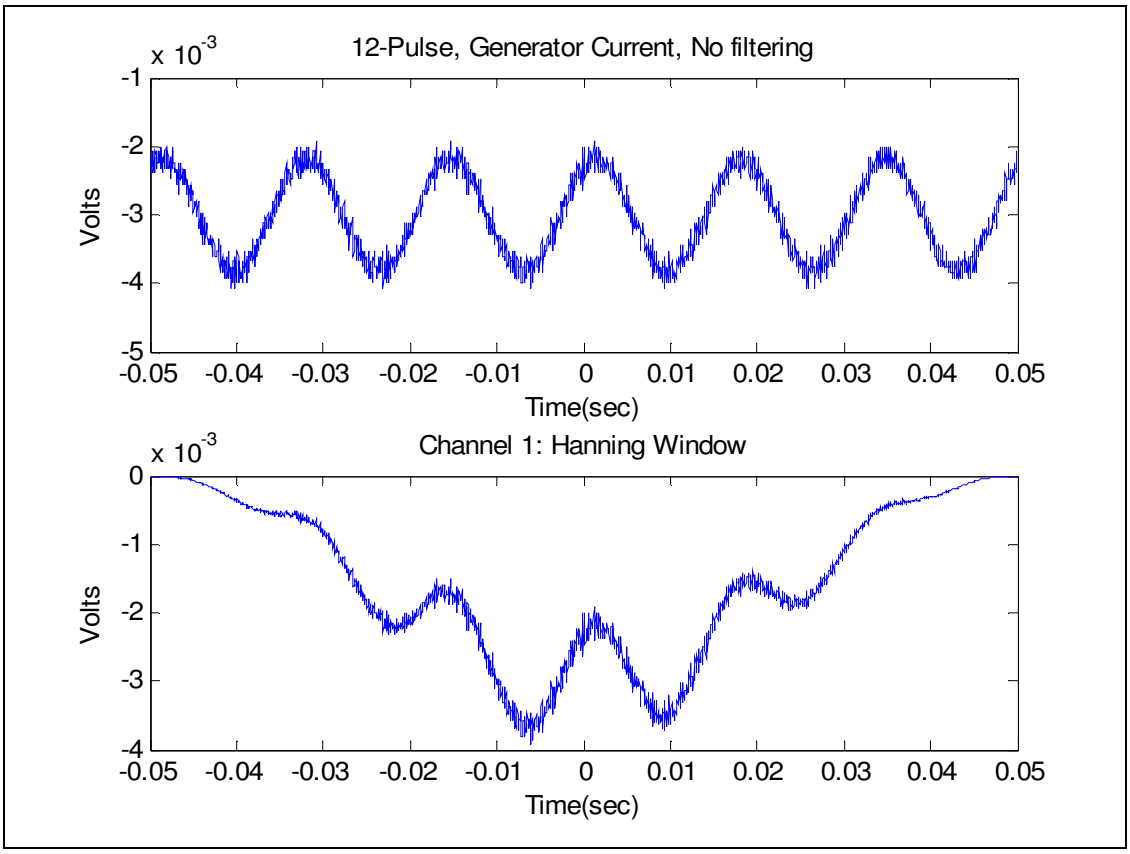

Figure 33: Generator Phase Current and Hanning Window

Although the THD could be extracted from the generator current, the large voltage drop prevented useful data from being collected. Through various troubleshooting techniques, the voltage drop was found to be due to larger internal resistances in the generator and transformer than initially anticipated. As a result, the hardware model of the twelve-pulse converter was abandoned and six-pulse converter data was taken using the variable power supply as an input voltage. The use of the variable power supply as the input voltage eliminated extraneous voltage drops cause by unexpected resistances. Future research might include finding a more appropriately sized generator for the twelve-pulse system.

D. Hardware Filtering

Hardware filtering was implemented through a system of AC motor-start capacitors and toroid-wound inductors. The inductors selected for the harmonic filters had a rated inductance value of 1.1mH. Capacitors were sized to tune the harmonic filters to the 5^{th}, 7^{th}, 11^{th}, and 13^{th} harmonic. The capacitors were also sized so to be placed in a delta configuration, since a delta configuration requires only a third of the capacitance of a Y configuration. In practice, at medium voltages (> 2.4 kV), the bank would be connected in Y to avoid line-to-line faults when a capacitor suffers dielectric failure.

Capacitors were then paired to the inductors in order to create a harmonic filter for the reduction of the desired harmonic. The inductors were measured and those selected for the actual harmonic filters had a value of 1.14mH. In the same manner, the capacitance of each capacitor was measured and only those with the closest value to the calculated capacitance were utilized. The following combinations of filtering were tested: no filtering, filters tuned to 5^{th} harmonic, filters tuned to 5^{th} and 7^{th} harmonics, and filters tuned to 5^{th} and 11^{th} harmonics. Table 6 lists the actual inductance and capacitance values used in the various hardware harmonic filters compared to the inductance and capacitance values of the filters designed in simulation. The filters modeled in simulation each contained an inductance of 1mH and a corresponding theoretical capacitance depending on harmonic number. Since capacitors from vendors are sized in ranges, the capacitors chosen for hardware had the closest capacitance value to the theoretical value.

Table 6: LC Values for Filtering

	Inductance (H)		Capacitance (F)	
Harmonic	Desired	Actual	Theoretical	Actual
5th	0.001	0.0014	9.3816E-05	9.20E-05
7th	0.001	0.0014	4.7865E-05	5.18E-05
11th	0.001	0.0014	1.9383E-05	2.20E-04

The filtering was built on a connector board, with the inductors and capacitors mounted on plastic housing that plugged directly into the board, as shown in Figure 34. The filtering tests were performed on the six-pulse thyristor system at the firing angles of 0°, 20.4° and 45°. A complete filtering solution with tuned filters to the 5^{th}, 7^{th}, 11^{th}, and 13^{th} harmonics was not possible due to Lab-Volt® limitations. With the filtering tuned to both the 5^{th} and 7^{th} harmonic, the power supply was already beginning to approach its rated value of current, restricting the ability to add more filtering.

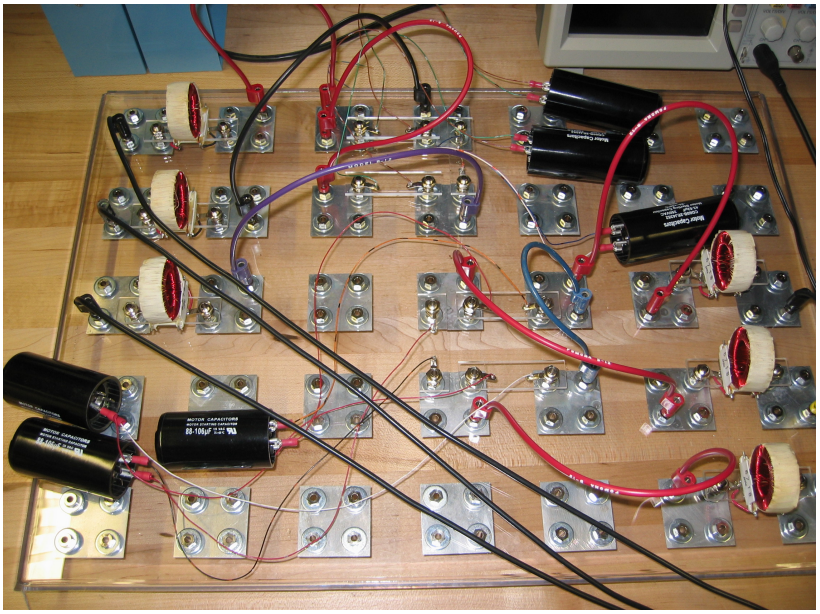

Figure 34: Implementation of Harmonic Filters on Connector Board

V. Comparison of Hardware to Simulation

Hardware and PSCAD® simulation comparison was performed on the six-pulse thyristor test system. The parameters of the hardware system were modeled as closely as possible in PSCAD®. The input voltage to both systems was $40V_{rms}$ line-to-neutral, or in the case of the hardware system, as close to 40V as possible. The THD results from hardware setup are an average of the THD results from the rectangular window and the Hanning window. The RMS phase current (I_a) for the software simulation is an estimate, using 0.7 times the peak value. Table 7 below shows the results between the hardware tests and PSCAD® simulations.

Table 7: Comparison of Hardware to Simulation Results for THD, V_{out}, and I_a

		V_{out} (V)		I_a RMS (A)		THD (%)	
Firing Angle (°)	Filtering	Hardware	Simulation	Hardware	Simulation	Hardware	Simulation
0.0	None	42.0	48.0	0.587	0.569	27.40	27.00
0.0	5th	45.1	46.9	2.819	2.541	8.48	4.42
0.0	5th,7th	43.7	45.8	4.013	3.710	6.92	2.33
0.0	5th,11th	41.8	46.3	3.300	2.982	8.20	3.63
20.4	None	28.1	44.4	0.464	0.483	34.59	45.30
20.4	5th	28.2	44.2	2.440	1.708	8.83	9.05
20.4	5th,7th	28.2	43.2	3.760	3.584	7.07	5.24
20.4	5th,11th	28.3	43.9	3.040	3.031	8.73	7.07
45.0	None	24.3	35.0	0.372	0.385	27.07	62.40
45.0	5th	24.7	34.5	2.460	2.170	8.39	8.90
45.0	5th,7th	24.6	33.4	3.750	3.430	6.78	4.86
45.0	5th,11th	24.8	33.2	3.080	2.835	8.43	6.27

The simulation had a tendency to underestimate the THD and phase current of the hardware six-pulse rectifier system, especially at operating points with phase delay. This may be due to such “real-world” effects as resistances and inductances inherent in wiring and the setup

of the hardware. Overall, the hardware data and simulation data were very similar, demonstrating that the simulation model can be validated by hardware results. Differences in output voltage can be attributed to voltage drops in the transformer, rectifier, and DC link inductors that become more prominent at low voltage.

Appendix B contains the waveforms collected from the hardware tests, as well as the full table of the THD values calculated by the rectangular and Hanning windows. The peak supply current values from the simulations are also shown in Appendix B.

VI. Tradeoff Analysis

Tradeoff analysis was assessed based on weight and harmonic performance of various rectifier system implementations. Within the scope of this project, tradeoff analysis considered the following propulsion drive options: Option A uses a six-pulse rectifier front end versus Option B, which uses a twelve-pulse rectifier front end. Both options include various combinations of harmonic filtering. The structure of the DC ship service distribution converter and the high-power radar converter are assumed to be at least 12-pulse rectifiers, due to the U.S. Navy's power quality requirements on the DC side of those loads.

Current surface combatant research assumes a propulsion drive rated on the order of 40MVA. As a consequence, the two options include the following components (per drive):

> *Option A*: one 40MVA phase-controlled rectifier; no transformer; filtering units
>
> *Option B*: two series-connected 20MVA phase-controlled rectifiers; two 20MVA three-phase transformers; filtering units

Smaller power electronic devices can be used in the 20MVA rectifier units; however, approximately twice as many devices are required (the need for redundancy and the lower voltage required for the twelve-pulse system makes this approximate), which doubles the number of snubber circuits, gate drives, and protection devices necessary. Thus on average, the aggregate of the two 20MVA rectifiers will be larger than the single 40MVA unit (precise vendor data is pending). In terms of weight, the most significant difference between the two options is the transformer. Option B requires two 20MVA transformers per propulsion drive with a net weight on the order of 100 tons (precise vendor data is pending). This large weight difference dwarfs the difference in the size of the rectifier units.

In sizing the generators and filter banks, it was assumed that sufficient filtering would be added to each respective system so that the phase-current THD of the generator would be identical each of the cases. If the generator experiences the same THD stress in both cases, then the same generator is admissible for operation. This is a pragmatic assumption, since the number of military-qualified generators is limited. Therefore, qualitatively, the six-pulse rectifier system will require substantially more passive filtering to achieve the same level of current THD as the twelve-pulse system.

To quantify the "cost" of filtering, harmonic filter data was assessed using data from the Northeast Power Systems, Inc. (www.nepsi.com) website. Data was available based on aggregate power factor correction kVAR (reactive power), the rated current of the filter, and the rated voltage. For a 4160V system and cancellation of only the 5^{th} harmonic, the data shown in Table 8 is relevant for harmonic filters with three steps in reactive power. The weight does not change appreciably for a variation in the total reactive power. In general, units with fewer steps (fewer LC combinations) weigh less while units with more steps weigh more.

The data for three steps is viewed as representative. To account for higher harmonics, the units would in general require less kVAR and smaller inductances. Thus, a 7^{th} harmonic filter or an 11^{th} harmonic filter should be smaller than the 5^{th} harmonic filter.

Table 8:Parameters for 3 Step, 5^{th} Harmonic Filter

Reactive Power (kVAR)	Weight (lbs)
710	14178
1421	14355
2131	14533
2841	14710
3551	14888
4262	15066
5683	15421

As the data indicates, if each filter required approximately six tons, then it would take the weight of over sixteen separate filters to be equivalent to the weight addition of the transformers in the twelve-pulse system, which still requires its own filtering.

As a result, based on weight, Option A with additional filtering will be more effective. In terms of THD performance, additional filtering of additional harmonics can make the six-pulse system equivalent to the twelve-pulse system. Thus the overriding determinant in the tradeoff analysis is the weight of the transformer. The conclusion must be that Option A should be used for shipboard propulsion as far as the problem is currently cast.

Option B can be made more attractive by shrinking the size of the transformer. This can be achieved through a higher frequency main AC bus (240Hz). While a higher frequency main AC bus will significantly bring down the weight of the transformer, it also introduces other technical issues. First, the issue of the availability of components at the frequency or the derating of 60Hz equipment to operate in a 240Hz environment (specifically switchgear) must be addressed. Second, U.S. manufacturers must be willing to build a small quantity of the specialized equipment with little other commercial market possibilities. Finally, large power high-frequency generators would need to be developed by the U.S. Navy and qualified for the marine environment. The assessment of a high-frequency alternative system could be an area of future research.

A final alternative to using the large 60Hz transformer would be to use high-voltage DC distribution from the main generators. This solution suffers from similar problems as the high frequency main AC bus system solution, specifically the need for specialized equipment and no real opportunities to leverage the commercial marketplace. However, this too can be an area of future research project.

VII. Conclusion

This project successfully demonstrated that the addition of filtering, along with multi-pulse converters can greatly reduce generator bus harmonics as measured by THD. A method of designing harmonic filters was introduced, demonstrating differences in the ability to reduce harmonics based on different choices for the values of inductance and capacitance. The process of optimizing the choice of inductance and capacitance was derived for a case when all rectifiers were operated at zero phase delay. The affect of varying the firing angle on thyristor rectifier systems with filtering was also explored, though source currents can become excessive if the zero delay angle values of inductance and capacitance are used. It was determined that if considerable phase delay is used, then the capacitors must be resized according to power factor correction or the capacitance values made adjustable. The ability of the designed harmonic filters to handle the greater harmonics associated with operating a thyristor system was also shown. The six-pulse simulation model in PSCAD® was verified by hardware results. A PSCAD® simulation of the full integrated power system was modeled, with the capability of simulating thyristor rectifier systems with various firing angles and various DC loads.

While the civilian ship industry has successfully realized Integrated Power System (IPS) architectures for ships, power density and acoustic requirements of the U.S. Navy are much more stringent. A successful, cost-effective implementation of multi-pulse rectifiers in combination with filtering to reduce power harmonics in an IPS would be extremely beneficial to the U.S. Navy in achieving its goal of an all-electric ship. The different implementations tested in this project will also allow the U.S. Navy to choose the best system based on the metrics considered. Even if the U.S. Navy decides to choose a different method of reducing harmonics, this project

still demonstrates the feasibility of improving power harmonics using multi-pulse converters and filtering and provides a methodology for evaluating future candidate architectures.

VII. Areas of Future Research

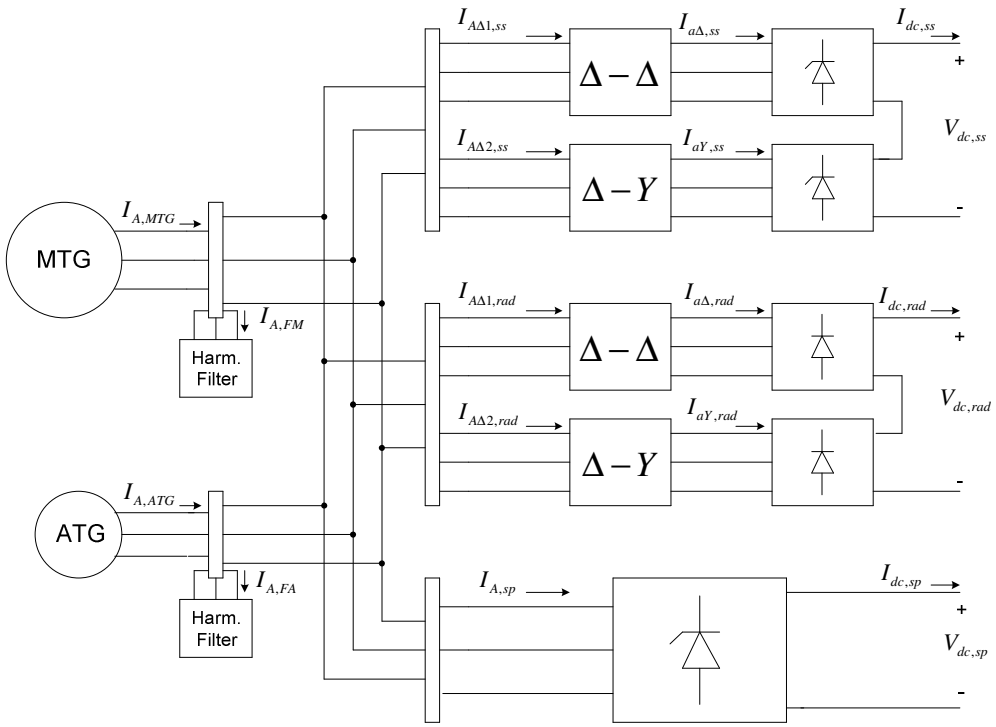

Figure 35: Integrated Power System Without DC Load

There are many aspects of harmonic filtering that have yet to be addressed. Future research could focus on the generator parameter known as sub-transient reactance. The machine sub-transient reactance impacts both potential fault current and voltage distortion. A minimum values is set by fault calculations; the maximum value is set by voltage THD requirements. Further research can explore the optimization of this value for an isolated generator or multiple units in parallel. Future studies could also focus on the DC side of the converter solution. Simulations run while varying of the DC side inductance demonstrated a change in the THD of the supply current; however, there did not seem to be a direct relationship between the DC inductance and THD. Follow-on work can explore the relationship between power quality on the DC load side versus THD on the AC side. This study focused solely on the LBES values for the

DC load of a warship. Varying other parameters may also lead to better system topologies for reducing THD. Acquiring and integrating a higher capacity generator into the hardware setup would facilitate improved data collection. The commercial industry also employs a step increment to filtering to gradually bring in reactive power in steps. The introduction of a stepped unit for filtering could change the method of designing filter values, as there are fewer concerns over the reactive power introduced by large capacitance values. Finally, future research efforts can expand the full-scale IPS model to represent the DC loads in more detail and consider multiple generators connected to a given bus.

---

[1] T. McCoy, "Trends in Ship Electric Propulsion". Power Engineering Summer Meeting, Vol.1, pp. 343-346, 2002.
[2] N. Doerry, J. Davis, "Integrated Power System for Marine Applications", *Naval Engineers Journal*, May 1994.
[3] "IEEE Harmonics in Power Systems", IEEE Std 141-1993, IEEE, New York, 1993.
[4] E. West, "Analysis of Harmonic Distortion in an Integrated Power System for Naval Applications", MIT, MSEE Thesis, 2005.
[5] N. Mohan, T.M. Undeland, W.P. Robbins, Power Electronics: Converters, Applications, and Design, John Wiley and Songs, pg. 39-42, 1989.
[6] Manitoba HVDC Research Centre, "Professional Power System Design and Simulation". Retrieved March, 2007. <http://www.pscad.com>.
[7] S.D. Sudhoff, S.F. Glover, B.T. Kuhn, "IPS FSAD Model Verification, Final Technical Progress Report". Energy Systems Analysis Consortium, 1999.
[8] "IEEE Recommended Practices and Requirements for Harmonic Control in Electrical Power Systems", IEEE Std 519-1992, IEEE, New York, 1993.
[9] LDS Group. "Understanding FFT Windows", 2003, Retrieved Nov, 2006. <http://www.lds-group.com/docs/site_documents/AN014%20Understanding%20FFT%20Windows.pdf>

VIII. Bibliography

1. Barton, T., Rectifiers, Cycloconverters, and AC Controllers, Clarendon Press: Oxford, 1994.
2. Bourguet, S., Guerin, P. & Le Doeuff, R., "Analysis of the Interharmonics Generated by a Ship Propulsion System", Presented at 11th International Conference on Harmonics and Quality of Power, 2004.
3. Cassimere, B., Rodriquez Valdez, C., Sudhoff, S., et al, "System Impact of Pulsed Power Loads on a Laboratory Scale Integrated Fight Through Power (IFTP) System", Presented at IEEE Electric Ship Technologies Symposium, 2005.
4. Ciezki, J. & Ashton, R., "Selection and Stability Issues Associated with a Navy Shipboard DC Zonal Electric Distribution System", *IEEE Transactions on Power Delivery*, Vol. 15, No. 2, April 2000.
5. Doerry, N., & Davis, J., "Integrated Power System for Marine Applications", *Naval Engineers Journal*, May 1994.
6. Electrotek Concepts., "Harmonic Studies", Retrieved Dec, 2006. <http://www.electrotek.com/harmonic.htm>
7. "IEEE Harmonics in Power Systems", IEEE Std. 141-1993, IEEE: New York, 1993.
8. "IEEE Recommended Practices and Requirements for Harmonic Control in Electric Power Systems", IEEE Std. 519-1993, IEEE: New York, 1993.
9. LDS Group. "Understanding FFT Windows", 2003, Retrieved Nov, 2006. <http://www.lds-group.com/docs/site_documents/AN014%20Understanding%20FFT%20Windows.pdf>

10. McCoy, T. & Dalton, T., "Design Implications of PWM Propulsion Motor Drives on Shipboard Power Systems". All-Electric Ship Conference, 1998.

11. McCoy, T., "Trends in Ship Electric Propulsion". Power Engineering Summer Meeting, Vol.1, pp. 343-346, 2002.

12. Mohan, N., Undeland, T.M. & Robbins, W.P., Power Electronics: Converters, Applications, and Design, John Wiley and Songs: New York, 1989.

13. Paice, D., Power Electronic Converter Harmonics, IEEE Press: New York, 1996.

14. Sudhoff, S.D., Glover, S.F., Kuhn, B.T., IPS FSAD Model Verification, Final Technical Progress Report. Energy Systems Analysis Consortium, October 1999.

15. Truong, L. & Birchenough, A., "Simulation and Analysis of Three-Phase Rectifiers for Aerospace Power Applications", Presented at Second International Energy Conversion Engineering Conference, Rhode Island, 2004.

16. West, E., "Analysis of Harmonic Distortion in an Integrated Power System for Naval Applications", MIT, MSEE Thesis, 2005.

IX. Appendices

A. Appendix A- MATLAB® Code

```
%This program extracts a waveform from an Tektronix TDS2024
%Oscilloscope and plots the waveform in MATLAB. It then calculates the
%FFT, which is plotted and calculates the THD.

%October 2006
%
%   This is the representation of an instrument control
%   session using a device object. The instrument control session
%   comprises all the steps to take when communicating with your
%   instrument. These steps are:
%       1. Create a device object
%       2. Connect to the instrument
%       3. Configure properties
%       4. Invoke functions
%       5. Disconnect from the instrument

% Create a GPIB object.
interfaceObj = instrfind('Type', 'gpib', 'BoardIndex', 0,
'PrimaryAddress', 4, 'Tag', '');

% Create the GPIB object if it does not exist
% otherwise use the object that was found.
if isempty(interfaceObj)
    interfaceObj = gpib('NI', 0, 4);
else
    fclose(interfaceObj);
    interfaceObj = interfaceObj(1);
end

%input buffer size
interfaceObj.inputbuffersize=1024;
interfaceObj.outputbuffersize=1024;

% Create a device object.
deviceObj = icdevice('tektronix_tds2024.mdd', interfaceObj);
connect(deviceObj)

% Extract waveform from Channel 1
waveform_group = get( deviceObj, 'Waveform' );
[y, t] = invoke(waveform_group, 'readwaveform', 'channel1');

% Delete objects.
fclose(interfaceObj);
disconnect(deviceObj);
delete([deviceObj interfaceObj]);
clear interfaceObj deviceObj;

%number of samples taken by o-scope
s=length(t);
```

```
%pick window out of Hanning, Hamming, or Blackman
graph=input('Window? (1-Hanning, 2-Hamming, 3-Blackman): ');
if graph==1
    w=hann(s);
elseif graph==2
    w=hamming(s);
elseif graph==3
    w=blackman(s);
end

w=w'; %changes from column vector to row vector

%sample frequency of o-scope
fs=1/((t(s)-t(1))/s);

y2=w.*y; %applies appropriate window

figure;
subplot(2,1,1);
plot(t,y)
xlabel('Time(sec)'); ylabel('Volts');
title('Channel 1: Rectangular Window');
subplot(2,1,2);
plot(t,y2)
xlabel('Time(sec)'); ylabel('Volts');
if graph==1
    title('Channel 1: Hanning Window');
elseif graph==2
    title('Channel 1: Hamming Window');
elseif graph==3
    title('Channel 1: Blackman Window');
end

%number of samples for fft
N=16384*4;

Y=fft(y,N);
Y2=fft(y2,N);

%useful frequency is only half
f=-N/2:N/2-1;
k=f*fs/N;

%frequency map and amplitude scaling
figure;
subplot(2,1,1);
plot(k, fftshift(abs(Y))/(s/2))
xlabel('Frequency(Hz)'); ylabel('Volts');
title('FFT: Rectangular Window');
subplot(2,1,2);
plot(k, fftshift(abs(Y2))/(s/2))
xlabel('Frequency(Hz)'); ylabel('Volts');
if graph==1
    title('FFT: Hanning Window');
elseif graph==2
```

```
    title('FFT: Hamming Window');
elseif graph==3
    title('FFT: Blackman Window');
end

 %extract values for harmonics
fund=60;    %fundamental frequency
n=1;
k2=round(k);%rounds fft frequency vector to nearest integer
c=[]; c2=[];       %vector of values for each harmonic frequency
d=[];       %vector of harmonic frequencies

z=fftshift(abs(Y))/(s/2);
z2=fftshift(abs(Y2))/(s/2);
counter=1;

while fund*n < max(k2)
    harm=fund*n;
    diff1=1;
    diff2=0;
    while diff1>=diff2 %finds closest data point to harmonic
        diff1=(harm-k(counter))^2;
        diff2=(harm-k(counter+1))^2;
        counter=counter+1;
    end
    b=z(counter-1);         %finds amplitude associated with harmonic
    b2=z2(counter-1);
    c=[c b];
    c2=[c2 b2];
    d=[d harm];
    %if length(d)>length(c) %if harmonic is not present, add 0 to value
    %associated with frequency
    n=n+1;
end

%calculate thd
num=0;
num2=0;
for n2=2:n-1,
    num=num + c(n2)^2;
    num2=num2+c2(n2)^2;
end
num=sqrt(num);  %sqrt of sum of harmonic amplitudes squared
num2=sqrt(num2);
denom2=c2(1);   %fundamental amplitude
denom=c(1);

THD_rectangular=num/denom

if graph==1
    THD_hanning=num2/denom2
elseif graph==2
    THD_hamming=num2/denom2
elseif graph==3
    THD_blackman=num2/denom2
End
```

B. Appendix B- Hardware/Simulation Data, Six-Pulse Current Waveforms

Table 9: Complete Hardware Simulation Data for Six-Pulse Rectifier

						THD (%)	
Firing Angle (°)	Filtering	Vin (V)	Vout (V)	Ia RMS (A)	Average THD (%)	Rectangular	Hanning
0.0	None	40.1	42.0	0.587	27.40	27.41	27.39
0.0	5th	40.6	45.1	2.819	8.48	8.48	8.48
0.0	5th,7th	39.4	43.7	4.013	6.92	6.93	6.9
0.0	5th,11th	40.0	41.8	3.300	8.20	8.22	8.18
20.4	None	40.1	28.1	0.464	34.59	34.54	34.64
20.4	5th	40.2	28.2	2.440	8.83	8.84	8.81
20.4	5th,7th	40.1	28.2	3.760	7.07	7.08	7.05
20.4	5th,11th	40.1	28.3	3.040	8.73	8.75	8.71
45.0	None	40.0	24.3	0.372	27.07	27.05	27.09
45.0	5th	40.4	24.7	2.460	8.39	8.41	8.37
45.0	5th,7th	40.4	24.6	3.750	6.78	6.77	6.79
45.0	5th,11th	40.6	24.8	3.080	8.43	8.42	8.43

Table 10: Complete PSCAD® Simulation Data for Six-Pulse Rectifier

Firing Angle (°)	Filtering	Vin (V)	Vout (V)	Ia RMS (A)	THD (%)	Ia peak (A)
0.0	None	40.0	48.0	0.569	27.00	0.813
0.0	5th	40.0	46.9	2.541	4.42	3.630
0.0	5th,7th	40.0	45.8	3.710	2.33	5.300
0.0	5th,11th	40.0	46.3	2.982	3.63	4.260
20.4	None	40.0	44.4	0.483	45.30	0.690
20.4	5th	40.0	44.2	1.708	9.05	2.440
20.4	5th,7th	40.0	43.2	3.584	5.24	5.120
20.4	5th,11th	40.0	43.9	3.031	7.07	4.330
45.0	None	40.0	35.0	0.385	62.40	0.550
45.0	5th	40.0	34.5	2.170	8.90	3.100
45.0	5th,7th	40.0	33.4	3.430	4.86	4.900
45.0	5th,11th	40.0	33.2	2.835	6.27	4.050

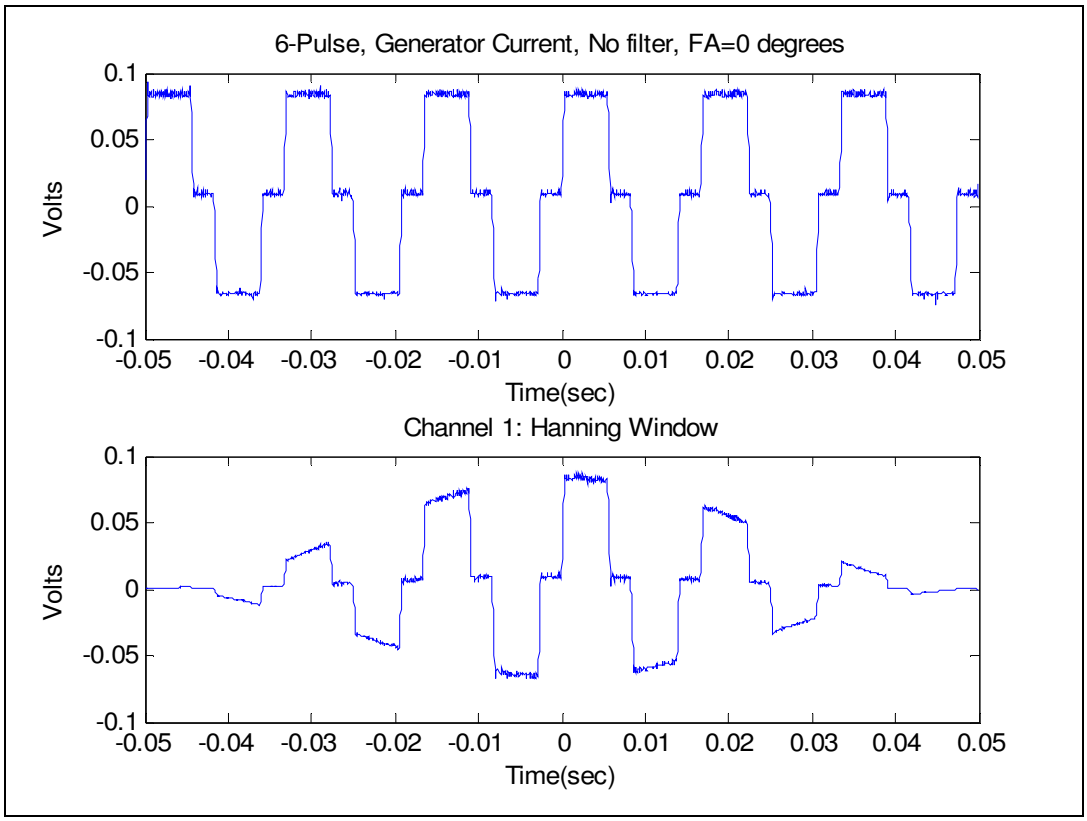

Figure B- 1: Generator Current for Six-Pulse, No Filter and Firing Angle=0°

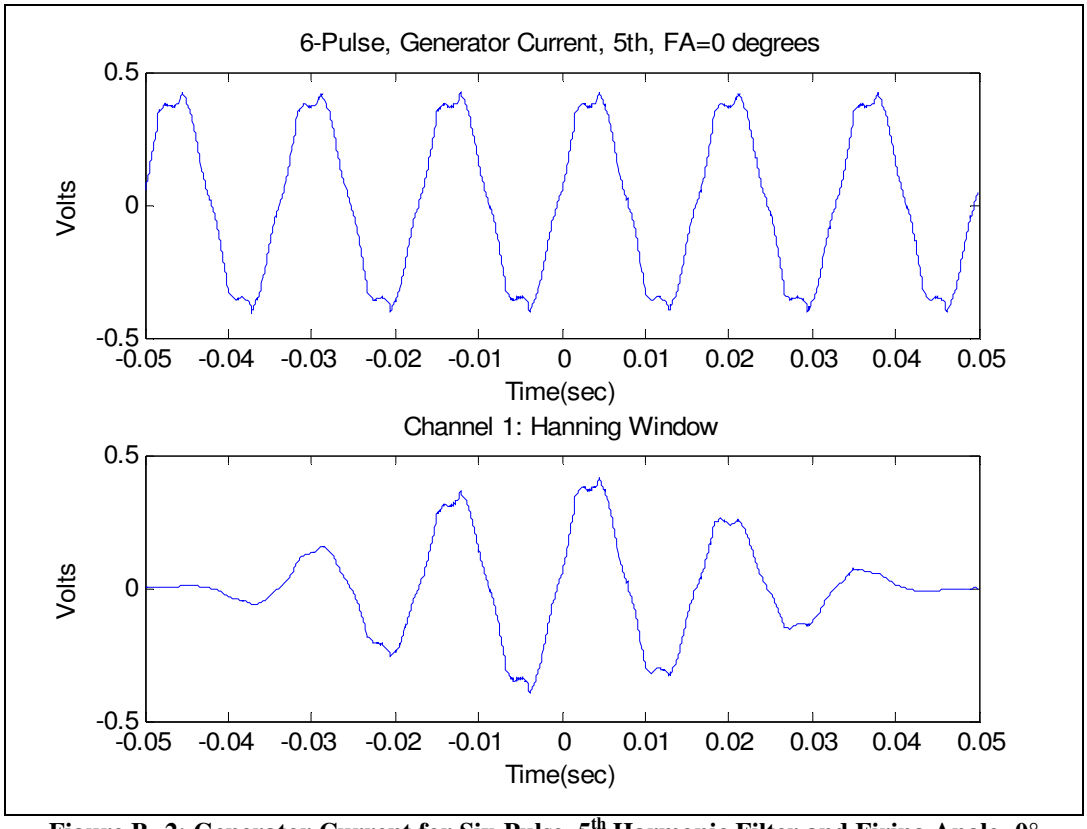

Figure B- 2: Generator Current for Six-Pulse, 5th Harmonic Filter and Firing Angle=0°

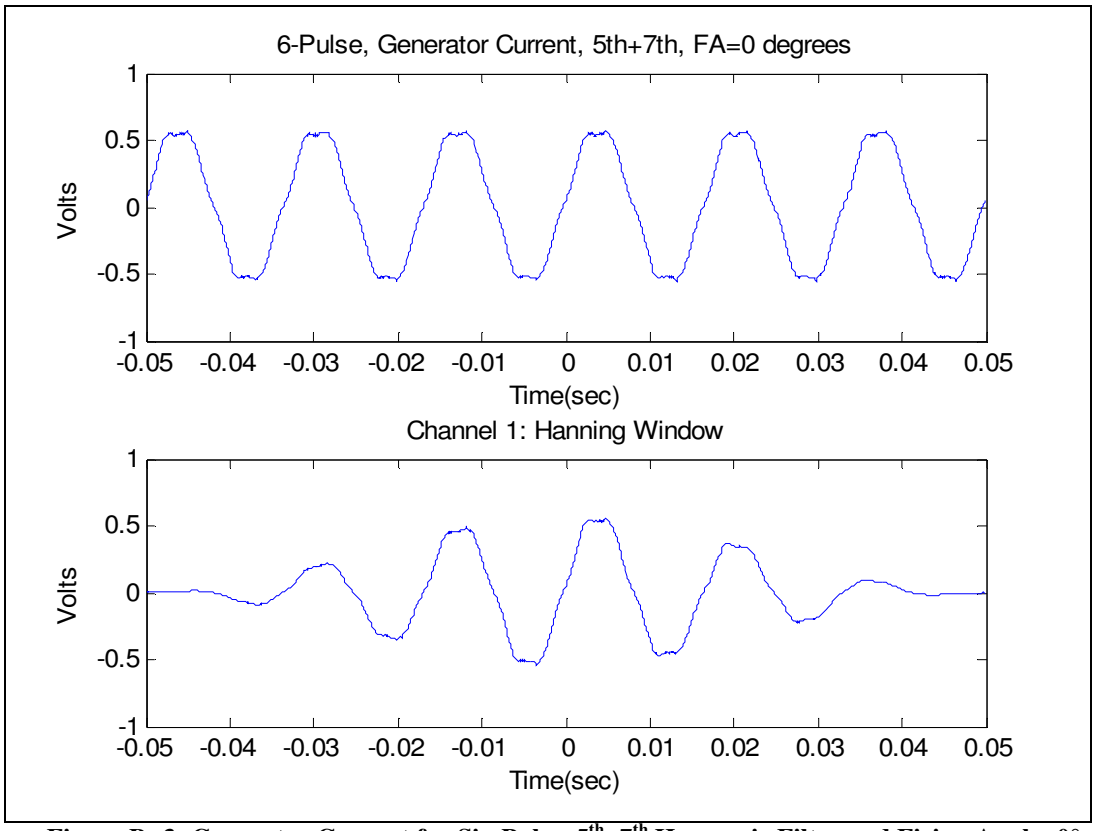

Figure B- 3: Generator Current for Six-Pulse, 5^{th}+7^{th} Harmonic Filter and Firing Angle=0°

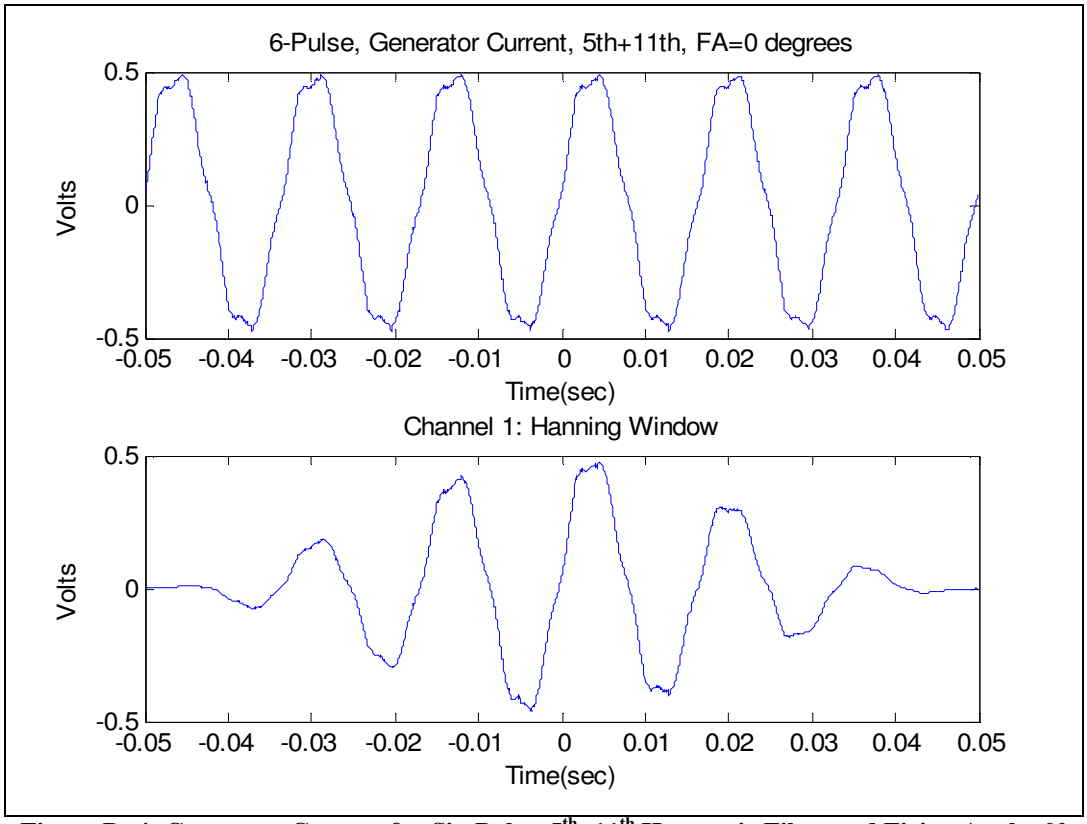

Figure B- 4: Generator Current for Six-Pulse, 5^{th}+11^{th} Harmonic Filter and Firing Angle=0°

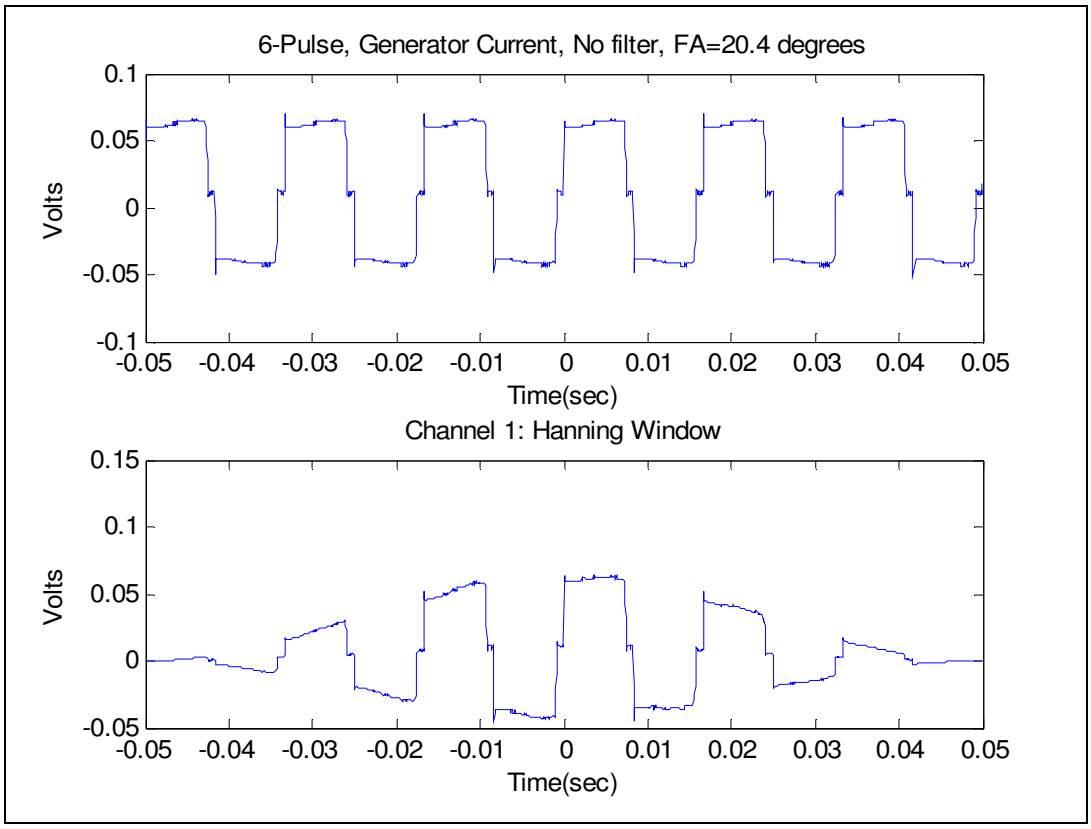

Figure B- 5: Generator Current for Six-Pulse, No Filter and Firing Angle=0°

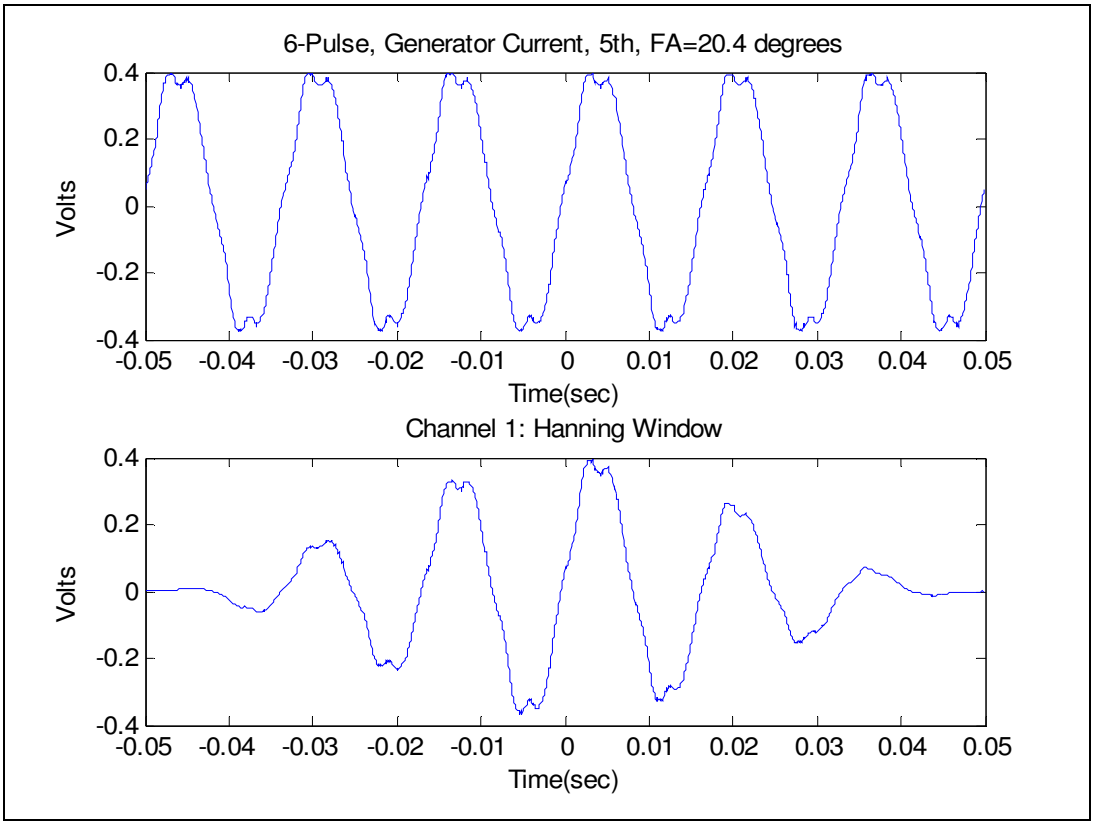

Figure B- 6: Generator Current for Six-Pulse, No Filter and Firing Angle=20.4°

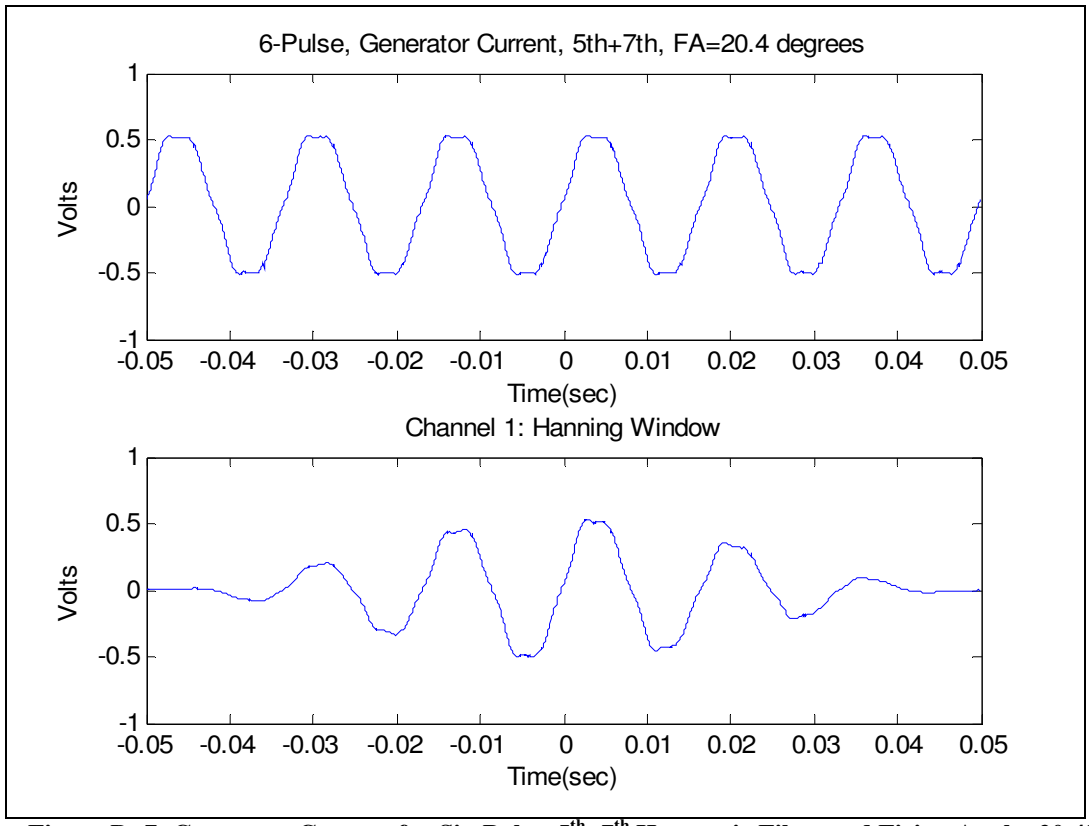

Figure B- 7: Generator Current for Six-Pulse, 5^{th}+7^{th} Harmonic Filter and Firing Angle=20.4°

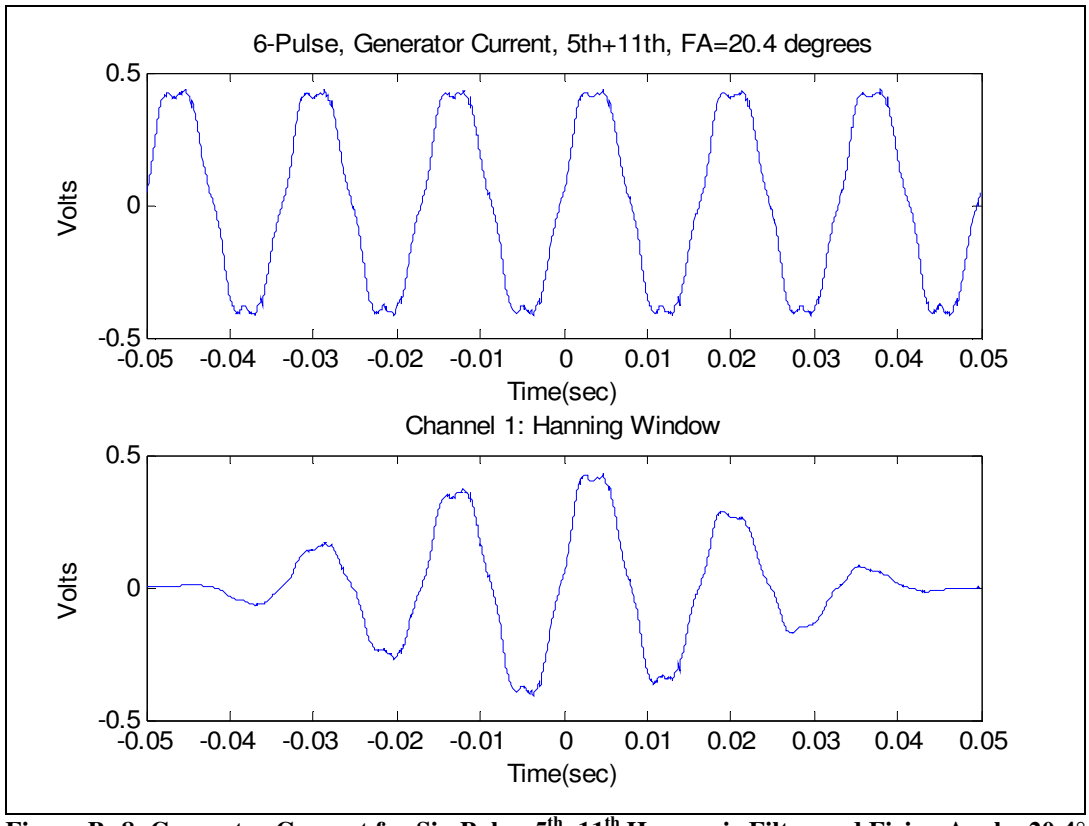

Figure B- 8: Generator Current for Six-Pulse, 5^{th}+11^{th} Harmonic Filter and Firing Angle=20.4°

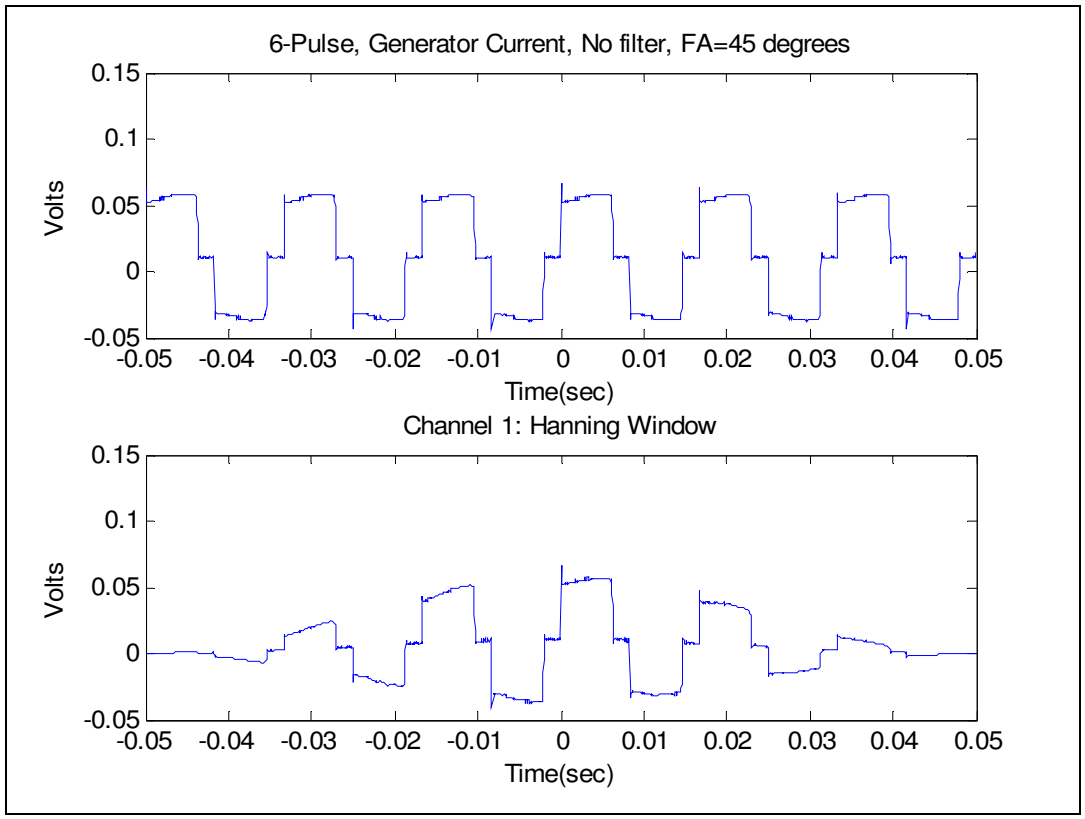

Figure B- 9: Generator Current for Six-Pulse, No Filter and Firing Angle=45°

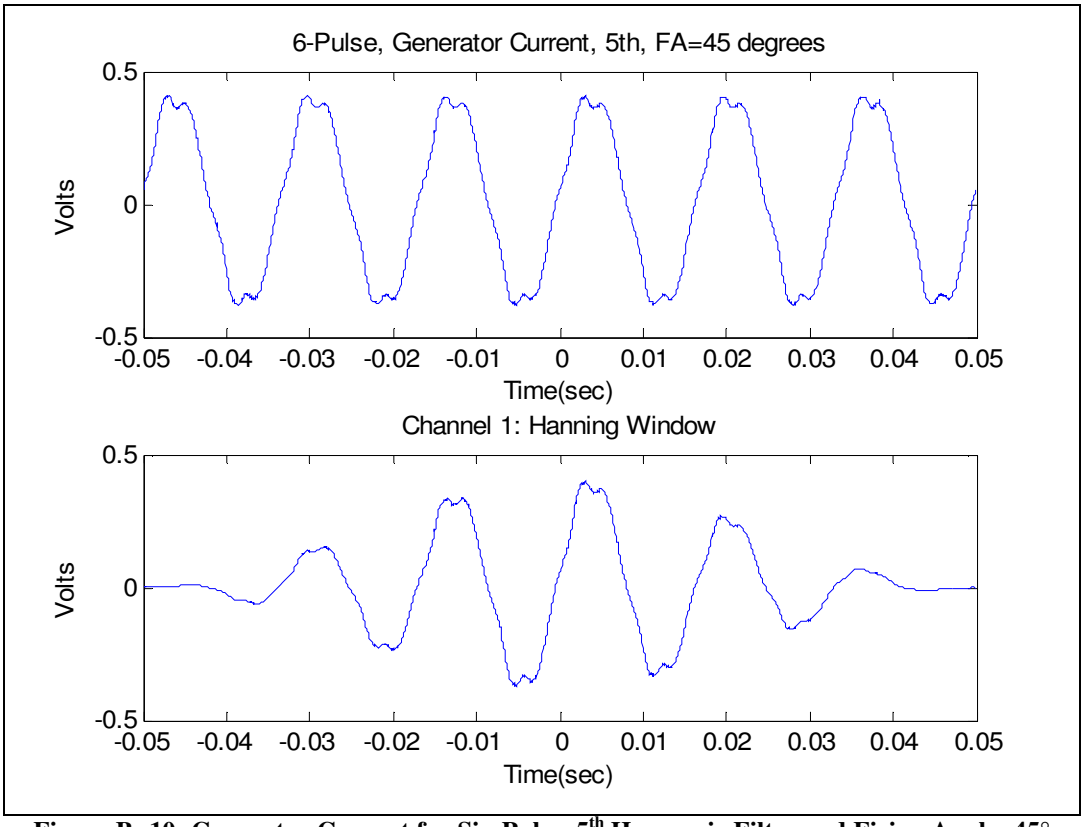

Figure B- 10: Generator Current for Six-Pulse, 5th Harmonic Filter and Firing Angle=45°

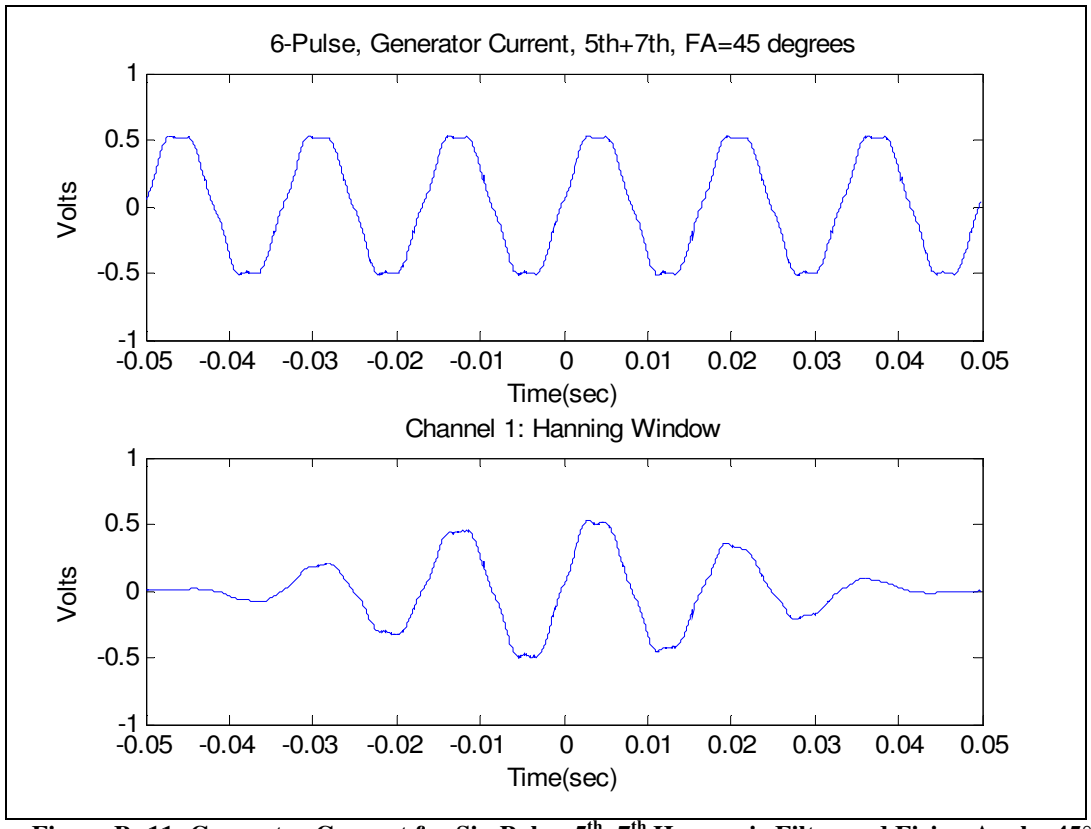

Figure B- 11: Generator Current for Six-Pulse, 5th+7th Harmonic Filter and Firing Angle=45°

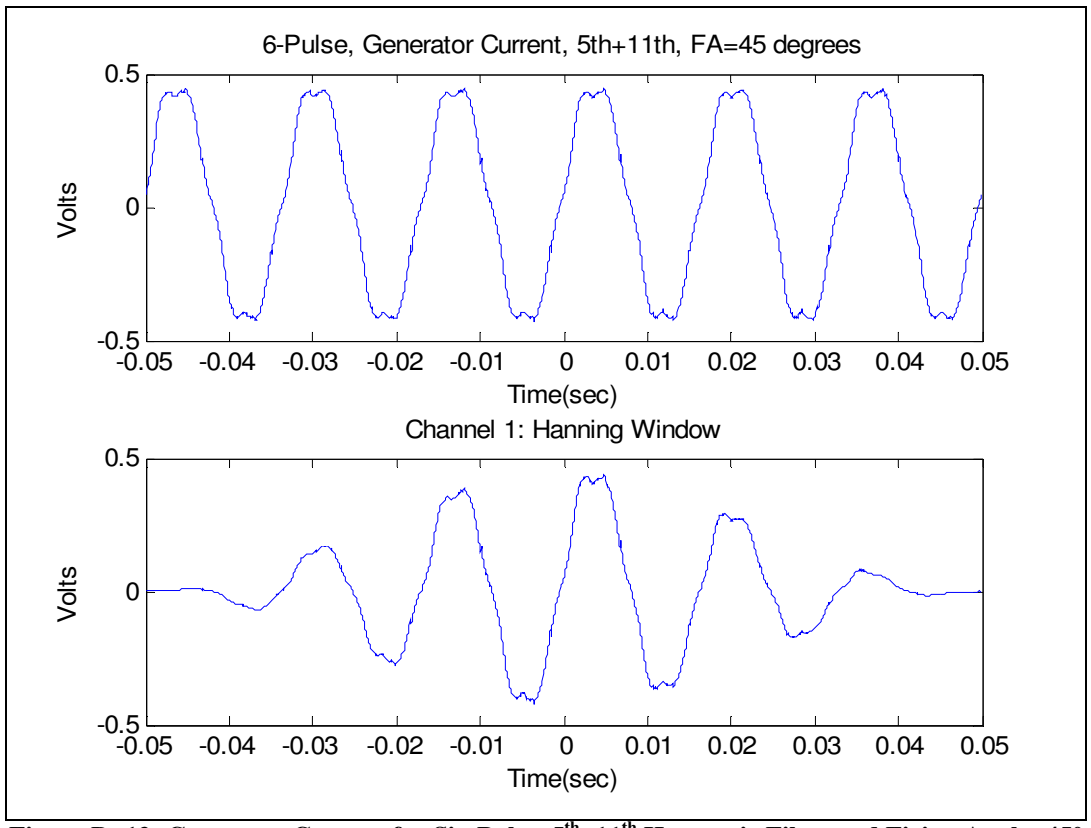

Figure B- 12: Generator Current for Six-Pulse, 5th+11th Harmonic Filter and Firing Angle=45°